بسم الله الرحمن الرحيم

Sudan University of Science and Technology

Faculty of Engineering

Aeronautical Engineering Department

Conceptual Design of Flapping Wing L.A.V

—Thesis Submitted in Partial Fulfillment of the Requirements for the Degree of Bachelor of Science. (BSc Honor)

By:

Hammam Azhary Hussein

Ibrahim Ahmed Omer

Mhamed Ali Jalaldein Mohamed Ahmed

Mohamed Hassan Sharafaldein

Sayed Mohmed Alhassan Alzubair

Supervised by:

Researcher. Mohamed Mahadi

Lec. Rania Qurashy

October,2016

ألاية

"أَوَلَمْ يَرَوْا إِلَى الطَّيْرِ فَوْقَهُمْ صَافَّاتٍ وَيَقْبِضْنَ ۚ مَا يُمْسِكُهُنَّ إِلَّا الرَّحْمَٰنُ ۚ إِنَّهُ بِكُلِّ شَيْءٍ بَصِيرٌ"

الملك - الآية 19

Abstract

This project presents the Conceptual Design of Flapping Wing L.A.V. Starting from a set of initial design specifications namely: weight, maximum flapping frequency and maximum and minimum velocity of the model. The model -aerodynamic surfaces and internal structure- was drawn using CATIA software. Then the aerodynamic forces were estimated analytically and with C.F.D methods for pure flapping motion.

Structure analysis was made through ANSYS software for the main components. The flapping mechanism was made and drawn depending on the movement angles to create enough lift and thrust resulted from C.F.D analysis.

The results of these analysis showed that: The maximum positive lift is created during down stroke phase, and vice versa the maximum negative lift is created during upstroke phase and Due to suitable and perfect material selection, there was no any redounded deformation in the structure and it can handle with the maximum load applied on it. These results prove that our model is able to generate required lift and thrust to fly without any failure.

During structure analysis with wing skin there was a problem of skweens being equal to one and this is not acceptable. This problem was solved by analyze the wing without skin.

التجريد

هذا المشروع يقدم تصميم أولي لمركبة جوية خفيفة ذات جناح رفراف . إبتداء من تشكيلة من المواصفات المبدئية للتصميم و هي: الوزن, والتردد الأقصى للرفرفة و السرعة القصوى و الدنيا للنموزج. السطوح الإيروديناميةو الهيكل الداخلي للنموزج رسمت بإستخدام برنامج (CATIA). ثم حسبت القوى الإيروديناميةتحليلياً وتحسيبياً بإستخدام نموذج(CFD) لحركة الرفرفة فقط.

التحليل الهيكلي للأجزاء الرئيسية تم بواسطة برنامج(ANSYS). آلية الرفرفة تم تصميمها و رسمها إعتماداً على زوايا الحركة لإنتاج الرفع و الدفع الكافيان و الناتجان من تحليل(CFD).

نتائج هذه التحليلات تبين أن: أقصى رفع موجب ينتج خلال شوط الهبوط, و العكس صحيح أقصى رفع سالب ينتج خلال مرحلة شوط الصعود و نتيجة للإختيار المناسب و المحكم للمواد, ليس هناك أي تشوه حرج في الهيكل الذي يمكنه التعامل مع أقصى حمل يطبق عليه. هذه النتائج تثبت أن النموذج قادر على توليد الرفع و الدفع المطلوبان للطيران من دون إخفاق.

خلال تحليل الهيكل بالغشاء الخارجي هناك مشكلة (skweens) الذي يساوي الرقم واحد و هذا ليس مقبول. هذه المشكلة تم حلها بتحليل الجناح من دون الغشاء الخارجي.

Acknowledgement

It is a pleasure to thank those who were supporting us during this project...

First, to ALLAH who created us …

To our families who built us to face this life …

To our inspired supervisor, Eng. Mohamed Mahadi …

To our great supervisor, Lec. Rania Qurashy

To researcher. Mohamed Al-tigani …

To our friends and colleagues …

To all staff of the Aeronautical Research Centre …

Dedication

اهدي هذا العمل المتواضع الى امي التي علمتني الصمود مهما تبدلت الظروف, التي لم تألُ جهدا في تربيتي وتوجيهي..

الى ابي الذي لم يبخل علي يوماً بشئ..الذي وهبني الحياة والعمل والنشأة على شغف الإطلاع والمعرفه..

الى اهلي وعشيرتي الأقربين..

الى اساتذتي الاجلاء..

الى اخي وصديقي الراحل المقيم احمد البخاري..

الى زملائي وزميلاتي..

الى الشموع التي تحترق لتضئ لنا الطريق..

اهديكم هذا البحث المتواضع راجياً من المولى عز وجل ان يجد القبول والنجاح...

Symbols

$\boldsymbol{m_M}$	Mass of model (kg)
b	Span (m)
I_m	Chord (m)
C_{amG}	Lift coefficient at glide
$C_{\Gamma G}$	Circulation characteristic number of the glide
C_{α}	Lift curve slop
$\boldsymbol{\alpha_0}$	Angle of attack for zero lift (rad)
σ	Setting angle (rad)
$C_{\Gamma 1}$	Circulation characteristic number of upstroke
$C_{\Gamma 2}$	Circulation characteristic number of Down stroke
k_v	Flight speed factor (ratio power to glide)
$\mathbf{t_p}$	Flapping period length (s)
$\boldsymbol{\Phi_E}$	Flapping angle ($\binom{+}{-}$meddle of stroke) (rad)
$y/_S$	Relative from the wing root
H	The distance from up and down stroke for the end of Internal spar inside the fuselage (m)
L_i	Length of internal spar inside the fuselage. (m)
θ_1	Required angle for internal spar (degree)
θ_2	Required angle for external spar (degree)

Abbreviations

LAV	Light Air Vehicle
CFD	Computational Fluid Dynamic
UAV	Unmanned Aerial Vehicle
PZT	Piezoelectric Transducer
ADAMS	Automated Dynamic Analysis Of Mechanical Systems
UDF	User Define Function
CAD	Computer Aided Design
PVC	polymer of Vinyl Chloride
D	Drag
HZ	Hertz
MAV	Micro Air Vehicle
NASA	National Aeronautics and Space Administration
Re	Reynolds number
C_L	Lift Coefficient
C_D	Drag Coefficient
W	Weight
T	Time
EW	External Wing
IW	Internal Wing
TVD	Total Variation Diminishing
SST	Shear Stress Transport
G	Gravity
VARTM	Vacuum Assisted Resin Transfer Molding
ES	External spar
IS	Internal spar

List of Content

Contents

List of Figures

List of Tables

1. Chapter One: Introduction

The preliminary design of conventional aircrafts started design with the assumption of cruising flights or trimmed flight conditions which require an aircraft to satisfy "the forces and moments equilibriums" without any continuous control efforts. For example, the weight of an aircraft is equal to the lift of the main wing, and the lift depends on the lift coefficient of the wing section (airfoil), the operating flight speed, and the wing area. The lift coefficient of a fixed-wing aircraft is proportional to the angle of attack.

Many aerodynamic researchers have designed various airfoils for specific mission requirements and tested them in wind tunnels to get the precise coefficients of lift, drag, and moments up to the stall boundary. [1]

If the energy cost is defined as the energy required to move one kilogram a distance of one kilometer, and plot it against the body mass of birds, terrestrial animals, and fish (Schmidt-Nielsen, 1972; Goldsping, 1977), one can see that for a given body size, running is the most expensive in terms of energy costs, while flying and swimming are the cheapest. This may be the main reason why nearly a million insect species and more than 9,000 warm blooded animals have taken to the skies. To counter the gravity force. [2]

A flapping wing aircrafts is a flight vehicle which generates aerodynamic forces and moments to fly and maintain its stability by a complex multi degree of freedom wing motion: flapping, pitching, twisting, and lagging. Therefore, flapping flight is more complicated than flight with fixed wings because of the structural movement and the resulting unsteady fluid dynamics.

The similarities between the aerodynamics of a flapping wing and that of a rotor craft, although limited, can illustrate a few key ideas. Take for example the rotors of a helicopter, which rotate about the central shaft continuously. The relative flow around the rotors produces lift. Likewise, a flapping wing rotates, swings in an arc around its shoulder joint, and reverses direction every half stroke.

Helicopters and biological flyers use similar techniques to accelerate from hovering to forward flight as well. Helicopters tilt the rotational plane of rotors from horizontal to forward. The steeper the tilt of the rotor, the faster the helicopters accelerates. Biological flyers also tilt their flapping stroke plane: down and forward on the down stroke, and up

and backward on the upstroke. To fly faster, biological flyers make the stroke more vertical by increasing the up-and-down aptitude of the movements. When biological flyers decrease their speed, they tend to flap their wings more horizontally, similar to the way helicopters change their rotors.[3]

The design of small flapping wing aircraft, there are too many design parameters including wing geometry, wing kinematics, and wing structural dynamics. The main difficulty during the design comes from the fact that we do not exactly know how each parameter affects the characteristics of the flapping wing aircraft system, especially its aerodynamics. [1]

For a bird to be able to deform and twist its wings, an adaptation in the skeletal and muscular systems is required. The key features that seem desirable are modification of camber and flexing of the wing plan form between upstroke and down stroke, twisting, area expansion and contraction, and transverse bending. To perform these functions, birds have a bone structure in their wings similar to the one in a human arm. Therefore, the bionic flapping wings get specially interest from researches because it can be better imitate the birds plunging and folding movement in flapping flight. [3]

Lift and thrust characteristics of flapping wing:

Simple flapping of wings with suitably chosen parameters, and overall light weight, can produce required lift and thrust.

Chunjin Yu, Daewon Kim, Yi Zhao studied lift and thrust generated by flapping motion using Three-dimension unsteady vortex lattice method and got the following observations:

1) Lift is mainly produced during down stroke; however, thrust is produced during both down stroke and upstroke.

The lift and thrust produced during down stroke are much more than that produced during upstroke.

2) Lift and thrust increase with the increase of flapping frequency

3) Thrust increases with the increase of flapping amplitude, but the lift decreases with the increase of flapping amplitude

4) Lift and thrust increase with the increase of mean pitching angle, but the effect on lift is much more than on thrust. [4]

The flapping theory first developed in the 1920's and 1930's by Von Karman, Garrick and Others, concerned to 2-D flat plates Oscillate in pitch and plunge. Garrick showed that a purely plunging flat plate can produce thrust, and the max efficiency is 50% (propeller max efficiency is 90%), but since 1990's researches concluded that the combined of pitching with plunging in 2-D can yield efficiency up to 90% important design parameters that effect flapping flight.

at NUST College of Electrical and Mechanical Engineering, Peshawar Road, Rawalpindi Pakistan the study the important design parameters that effect flapping flight and the result was:

a). Lift of an ornithopter is most influenced by the incidence angle and forward speed but least affected by flapping frequency.

b). Thrust of an ornithopter is most affected by flapping frequency and forward speed but least influenced by incidence angle.

c). The drag force increases with increase in forward speed, incidence angle, and flapping frequency.

d). The increase in total flapping angle, increases all the forces but the effect is marked on drag force

1.1 Aim and Objectives

Aim: The project aims to boost scientific research in science of developing aeronautical synthetic materials or structures that behave similar to biological systems, in the college and other country universities.

1.2 Objectives

- Discuss fixed wing problems in low Reynolds number region.
- Study the flapping wing theorems as a solve for above problem
- Apply flapping wings theorems on a useful object.

1.3 Problem statement

In some missions, -like surveillances, reconnaissance, indoor flight and wildlife control-, there is need to fly in low Reynolds number regions, which is the region of the natural flyers flying, while the other types of wing are not efficient in this regions.

1.4 Proposed solution

By using the concept of the propulsion that found in nature, design an aircraft with wing which generates both lift and thrust.

1.5 Methodology

Starting from Data collection, the design requirements were specified and hence A/C configuration was drawn. Aerodynamics characteristics were estimated analytically and computationally and matched with the structure configuration computationally. Structure analysis was done. And mechanism was designed according to the aerodynamic result and system selection was made.

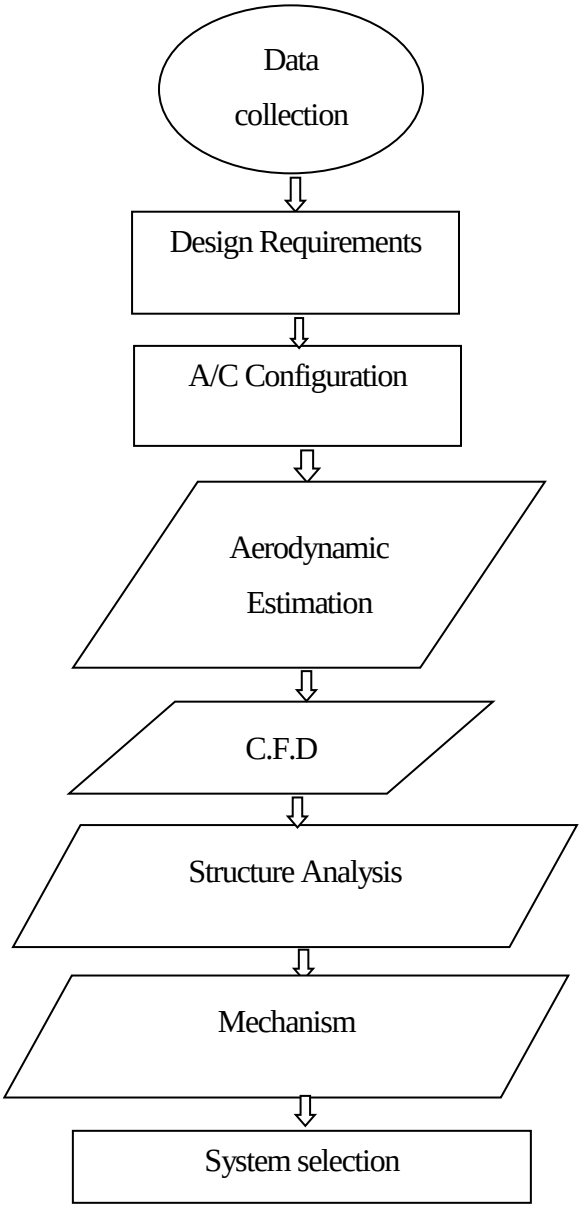

1.6 Methods and Tools

- Using CATIA to draw the configuration
- Analytical solution for aerodynamic
- Using ANSYS software for CFD and structure design.
- MATLAB

1.7 Thesis outline

- Chapter one is an introduction.
- Chapter two presents literature review.
- Chapter three presents aerodynamic estimation, structure analysis and mechanism design.
- Chapter four includes results and discussion.
- Chapter five presents conclusion, recommendation and future work.

2 Chapter Two: Literature Review

Need for the development of an ornithopter is based on the argument that flapping wing flight, at small scale, is more efficient than traditional fixed wing and rotary flight.

Flapping wing flight more closely mimics natural flight and has potential for being lower in weight and having greater endurance. In addition, strategic and stealth applications for flapping wing vehicles are evident as well, as they mimic natural flyers and could steal their presence. Thus, flapping wing air vehicles may provide a significant advantage over their fixed-wing counterparts especially

in tactical military applications.

It has been shown that flapping wing based UAVs have certain advantages compared to their fixed wing counterparts:

1) Ability to hover reacts more efficiently to gusts, have lower weight, and generate lift without excessive size and weight.

2) Flexible wings have also been shown to be more advantageous than rigid wings, with having higher stall angles by performing adaptive washout, and providing

smoother flight.

3) The main advantage of flexible wings is that they facilitate shape adaptation, essentially adapting to the airflow to provide a smoother flight. A wing changes

shape as a function of angle of attack and wind speed. This adaptive washout is produced through extension of the membrane and twisting of the structural members, resulting in angle of attack changes along the span of the wing in response to the oncoming flow.

From early times, the idea of utilizing the thrust generated from flapping wings for man-made flying vehicles emerged from observations of birds. One of the first attempts to explain and implement the mechanism of thrust generated from flapping wings to a flying vehicle was made by Leonardo da Vinci. During the second half of the 20^{th} century, research on flapping wing propulsion intensified, fueled by the fact that numerous biological organisms using flapping wing propulsion (in air or in water) possess superior aero-hydrodynamic properties.

Energy cost is the energy required to move one kilogram a distance of one kilometer, and plot it against the body mass of birds, terrestrial animals, and fish (Schmidt-Nielsen, 1972; Goldsping, 1977), one can see that for a given body size, running is the most expensive in terms of energy costs, while flying and swimming are the cheapest. This may be the main reason why nearly a million insect species and more than 9,000 warm blooded animals have taken to the skies. To counter the gravity force. [2]

Flapping aircraft will fill the space left by conventional fixed wing and rotary wings in term of maneuverability and aerodynamic efficiency when operating at low Reynolds numbers. [5]

Typical example of the early design of flapping vehicles can be seen in the sketches of da Vinci and Cayley. It seemed that the flapping flying machines were being forgotten with the great success of fixed wing aviation.[3]Presently the most famous flapping aircraft is "SmartBird" and "Snow Bird".

Smart Bird is an ultralight but powerful flight model which is managed by FESTO Company in Germany and its first flight done in 2011, it has excellent aerodynamic qualities and bionic technology-bearer, which is inspired by herring gull with wingspan of 2m, and can start fly and land autonomously. Its wings not only beat up and down, but also twist at specific angles which in conjunction with a complex control system make for first time in realizing an energy-efficient technical adaption of the natural model.

The Snowbird is the first human-power ornithopter designed by the University of Toronto in Canada and its best sustained flight occurring on 2011. It has a wingspan of 32m and best flapping frequency of 0.65Hz, but its significant design feature is that the wing contains no hinge mechanism; the flapping motion is articulated through the flexibility of the spar itself. The pilots legs transfer the leg-press motion to the wings with cables, each press translates into the downstroke of the wings, and the recovery of the wings are drawn up by the aerodynamic forces and the elastic forces in the spar, required no power from the pilot. [6]

The typical design of new air vehicles refers to existing baseline models, in the case of flapping air vehicles, the base line model can be found in nature. In order to development of successful flapping UAV the following items should be considered:

- An efficient aerodynamic model for low Reynolds number flow.
- Design considering fluid-structure interaction.
- Bio-inspired design of flapping-wing motion mechanism.
- Robust flight navigation and control.
- Miniaturized electronics and a micro power source

Note all above issues usually linked to each other. The preliminary design and Aerodynamic model of flapping UAVs is different from those of conventional aircraft. The design of fixed and rotary-wing aircrafts start with the assumption of trimmed flight conditions which require an aircraft to satisfy the forces and moments equilibriums without

any continuous control efforts, but a flapping wing aircrafts maintain its stability by a complex multi degree of freedom of wing motion: flapping, pitching, twisting and lagging.[1]

Flapping UAV design can be categorized into bird types (correspond to aircraft called Ornithopter) and insect type (correspond to aircraft called Entomopter), this category is according to:

Wing actuation mechanisms: This can be motor actuation linkage or PZT impalement vibro-actuation.

Aerodynamic mechanisms: which can be quasi steady (which applied to high aspect ratio wing and slow flapping motion) and unsteady. But the systematic design of flapping UAVs will not be possible without deep understanding of unsteady aerodynamic mechanisms, therefore a simpler or reduced-order unsteady aerodynamic model is used in the design.

The preliminary design of a biologically inspired flapping UAV start from a set of initial design specifications, namely: weight maximum flapping frequency and the minimum hand-launch velocity of the model. The model shape, size and flight conditions are usually chosen to approximate those of a certain bird closely meets the design specifications. The wings used are a simplification of the actual wing, where the wing surface coordinates is extracted using 3D laser scanner [by liu et al]. The fuselage is designed to produce low drag and has a low negative contribution to overall stability of the model, and a few design approximations are made. [5]

The aerodynamic research tools that can be used for flapping flight research are:

- Observation of biological example.
- Aerodynamic theory, including simulation.
- Wind tunnel experiments
- Flight testing

The flapping theory first developed in the 1920's and 1930's by Von Karman, Garrick and Others, concerned to 2-D flat plates Oscillate in pitch and plunge. Garrick showed that a purely plunging flat plate can produce thrust, and the max efficiency is 50% (propeller max efficiency is 90%), but since 1990's researches concluded that the combined of pitching with plunging in 2-D can yield efficiency up to 90%.

To full study the flapping theory the 3-D effects must be taken in account, the first reason is the plunging speed is not the same along the wingspan; the wing tip move faster than the wing root, in result the main generation of thrust is in the outer part of the wing and the lift in the inner part of the wing. In addition, the flapping wings have different trailing edge pattern depended on its gait.

Analytical unsteady aero theory does not exist; numerical theory is borrowing from aero elasticity;

- Vortex-lattice approach
- Source-doublet method

In the university of Liege in Belgium a wind tunnel model called " Frankenbird" is used to study the flapping wing aerodynamics, with the specifications: Duck (medium size), wingspan=1.3m, aspect ratio=8.6, am angle =+/-30 degree, pitch angle=+/-15 degree, its result show that when maximum thrust is produced the lift is also maximum, on the other hand drag generated when the lift is low. [7]

The down stroke produces a lot of lift and thrust, and the upstroke generates mainly drag and little lift. The lift coefficient value is are sensitive to the changes of the Reynolds number, airfoil, aspect ratio and the plunging and pitching of the wing. [3]

Thrust can be generated when flapping and leading pitching only, when the effective angle of attack is small, and the flow remain attached at all times. Unfortunately, we can't get high lift and high thrust at the same time, because high lift occurs when the flow allowed to separate (dynamic stall), therefore pitch leading must use for cruise, and dynamic stall for takeoff and rapid climb.[7]

In order to development of bio-inspired flapping structure many researches are made, but the bionic flapping wings get specially interest because it can be better imitate the birds plunging and folding movement in flapping flight. The prototype of flapping-wing mechanism is established, while kinematics simulation is implemented using ADAMS software, with dynamic grids technology to do the numerical simulation of unsteady flow around the bionic wing model with fluent analysis software and the lift curve is got. The simulation results show that using symmetric flapping-wing mechanism can get a larger lift and meet the requirements of the bionic flapping wing flight. [8]

The study of flapping wing motion to understand how birds and insect fly and how they produce lift and thrust is one of the most challenging things in the world of aerodynamics

The field is characterized by unsteady aerodynamics, whose knowledge is still developing. Birds and insects have different methods of producing lift and thrust for hovering and forward flight. Simple flapping of wings with suitably chosen parameters, and overall light weight, can produce required lift and thrust. Thus most of the successful ornithopters are designed only with flapping mechanism having flexible membrane wings. The flexibility of the wings causes passive pitching movement during flapping which improves the performance. Flapping frequency, flapping amplitude, incidence angle, flexibility of wings and their geometry are the important design parameters for an ornithopter**.**

2.1 Important design parameters that effect flapping flight:

At NUST College of Electrical and Mechanical Engineering, Peshawar Road, Rawalpindi Pakistan the study the important design parameters that effect flapping flight and the result was:

a). Lift of an ornithopter is most influenced by the incidence angle and forward speed but least affected by flapping frequency.

b). Thrust of an ornithopter is most affected by flapping frequency and forward speed but least influenced by incidence angle.

c). The drag force increases with increase in forward speed, incidence angle, and flapping frequency.

d). The increase in total flapping angle, increases all the forces but the effect is marked on drag force. [9]

A generic approach is carried out to model the kinematics and aerodynamics of ornithopter to mimic flapping wing to produce lift and thrust for hovering and forward flight, by considering the motion of a three-dimensional rigid thin wing in flapping and pitching motion with phase lag. Basic Unsteady Aerodynamic Approach incorporating salient features of viscous effect and leading-edge suction will be utilized. Parametric study is carried out to reveal the aerodynamic characteristics of ornithopter flight characteristics and for the analysis of various selected simple models in the literature, in an effort to develop a flying ortnithopter model. Further considerations will be given to other important parameters such as flapping frequency and wing geometry for well conceived formulations with realistic and workable assumptions and limitations. The present work has been performed to assess the effect of flapping-pitching motion with pitch-flap phase lag in the flight of ornithopter. In this conjunction, a computational model has been considered, and a generic computational procedure has been adopted. Two-dimensional unsteady

theory of Theodorsen with modifications to account for three-dimensional and viscous effects, leading edge suction and post-stall behaviour. The study is carried out on rectangular and semi-elliptical wing planforms. The results have been compared and validated with others within similar unsteady aerodynamic approach and general physical data, and within the physical assumptions limitations, have encouraging qualitative agreement or better. Judging from lift per unit span, the present flapping-wing model performance is comparable to those studied by Byl and Malik et al, while DeLaurier s pterosaur model is order of magnitude larger and comparable to Bald Eagle.

The analysis and simulation by splitting the flapping and pitching motion shows that:

(a) The lift is dominantly produced by the pitching motion, since the relative airflow effect prevailed along 75% of the chord length.

(b) The thrust is dominated by flapping motion. The vertical component of relative velocity increases significantly as compared to the horizontal components, which causes the force vector produced by the flapping-pitching motion to be directed towards the horizontal axis (thrust axis).

(c) The drag is dominated by the flapping motion, due to higher relative velocity as well as higher induced drag due to circulation.

A structured approach has been followed to assess the effect of different design parameters on lift , thrust, and drag of an ornithopter, as well as the individual contribution of the component of motion.

These results lend support to the utilization of the generic modelling adopted in the synthesis of a flight model, although more refined approach should be developed. Various approaches for ornithopter aerodynamic modelling could be followed, such as the incorporation of other parameters, and the use of more refined blade element, CFD or lifting surface methods. In retrospect, a generic physical and computational model based on simple kinematics and basic aerodynamics of a flapping-wing ornithopter has been demonstrated to be capable of revealing its basic characteristics and can be utilized for further development of a flapping-wing MAV. [10]

An experimental study was conducted to assess the aerodynamic benefits of flapping flight compared with fixed-wing soaring flight for the development of flapping-wing Micro-Air-Vehicles (MAVs). The time-averaged aerodynamic performance (i.e. mean lift and thrust/drag) of two flexible membrane wings with different skin flexibilities (i.e., a flexible nylon wing and a more flexible latex wing) were compared with that of a conventional rigid wing in order to assess the effects of skin flexibility of the tested wings on their aerodynamic performances. Advance ratio, which is defined as the ratio of the forward flight speed to the wingtip velocity of the tested wings in flapping flight, was used to do the data reduction to characterize the aerodynamic advantages of flapping flight over soaring flight.

The measurement results revealed clearly that flapping motions could bring significant aerodynamic benefits when the flapping flight is in an unsteady state regime with advance ratio $J < 1.0$. Both lift and thrust augmentations due to flapping motion were found to decrease exponentially as the advance ratio increases, the aerodynamic advantages of flapping flight would diminish rapidly

With the increasing advance ratio. Flapping motion could even become detrimental for high speed flight applications. The orientation angle of the flapping motion with respect to the incoming flow velocity was found to have considerable effects on both the lift and thrust generation of the tested wings in flapping flight. More lift was found to be generated as the orientation angle of the flapping motion increases in general. The tested wings were found to produce maximum thrust when the orientation angle was zero. The thrust generated due to flapping motion would decrease monotonically with the increasing

orientation angle. The skin flexibility of the tested wings was found to affect their aerodynamic performances significantly for both soaring flight and flapping flight. [11-15]

2.2 Wing Motions

Azuma (1992) identified four fundamental motions of a beating wing:

1. an out-of-plane motion called “flapping” (flapping angle ψ);

2. an in-plane motion called “lagging” (lag or azimuthal angle ζ);

3. a twisting motion of the wing pitch called “feathering” (feathering angle θ);

4. an alternatively extending and contracting motion of the wingspan called “spanning.[2]

lift and thrust generated by flapping motion using Three-dimension unsteady vortex lattice method:

Simple flapping of wings with suitably chosen parameters, and overall light weight, can produce required lift and thrust. Chunjin Yu, Daewon Kim, Yi Zhao studied lift and thrust generated by flapping motion using Three-dimension unsteady vortex lattice method and got the following observations :

1) Lift is mainly produced during down stroke; however, thrust is produced during both down stroke and upstroke.

The lift and thrust produced during down stroke are much more than that produced during upstroke.

2) Lift and thrust increase with the increase of flapping frequency

3) Thrust increases with the increase of flapping amplitude, but the lift decreases with the increase of flapping amplitude

4) Lift and thrust increase with the increase of mean pitching angle, but the effect on lift is much more than on thrust. [4]

There are many configurations and design process of flapping wing LAV corresponds to

design of a biologically inspired flapping UAV. Starting from a set of initial design specifications from a real bird, namely: weight, maximum flapping frequency and the minimum hand-launch velocity of the model as Joel E. Guerrero, Carlo Pacioselli , Jan Oscar Pralits, Francesca Negrello , Paolo Silvestri and Alessandro Bottaro did in their scientific paper.

They were lucky in choosing selig 1223 airfoil because of its thickness and extreme camber which can be very helpful in the aerodynamic of low RE and can produce high aerodynamic efficiency and that why choose it for our model. But we think that the gaps

at part connections must be recovered because it is a kind of ineffective area which can cause downwash.

Or four-flapping wing design utilizing the clap-and-fling effect , allows for the design of a vehicle capable of flight with a simplified wing motion Because the wing movements of most birds and insects is very complex with twists and other motions that are not yet fully understood by experts , as James Nicolora , Daniel Pappas , Luke Sorensen did in their scientific paper.

The equation they used to calculate the generated lift was not suitable because it is used only for rectangular wing , also the value of C_L was assume to be 1 and that was not the true value (0.8), these two assumptions decreased the accuracy of lift value.

3 chapter three: Flapping Wing LAV Design

On this chapter an in-depth analysis of the LAV is achieved. The configuration has been extracted from the bird actually that has the Arabic name NAWRAS, so our named UAV is NAWRAS LAV, we are trying on this project to design a simulated mechanism as the bird actually, every one come to know that birds feathered and glides by nature, but after depth analysis we can say that the nature prediction and simulation is the hardest point on this research.

The model specification is as in table 1.

Table 1 Model specification

Maximum weight	9.8 N
Maximum flapping frequency	3.0 Hz
Minimum velocity (hand launch velocity)	5.0 m/s
Maximum velocity	14.0 m/s

3.1 Aerodynamics

3.1.1 Aerodynamic design

The aerodynamic design of flapping wing LAV is very difficult that it is low Re number aerodynamic and unsteady aerodynamic so there is must consider the both of them in the design proses and they affect every piece of the aircraft and the design parameter.

3.1.2 airfoil selection

The airfoil selection is one of most important design parameter in aerodynamic estimation of aircraft that is effect the lift generation and stability characteristic of the aircraft.

The airfoil section of the design must be low Re number and high lift and high stall angle that flapping wing due to flapping produce high angle of attack in positive and negative during the up and down motion. The preferred low Reynolds number airfoil

shapes are different from those typically used for manned aircraft in thickness, camber, and AR

For this reason, the best airfoil is S1223 airfoil with stall angle higher than 20 degrees and zero lift angle -13 degrees and CL/CD higher than 65 and lift at zero angle is with CL =1.5 for all this S1223 airfoil is the airfoil that we chose for our design.

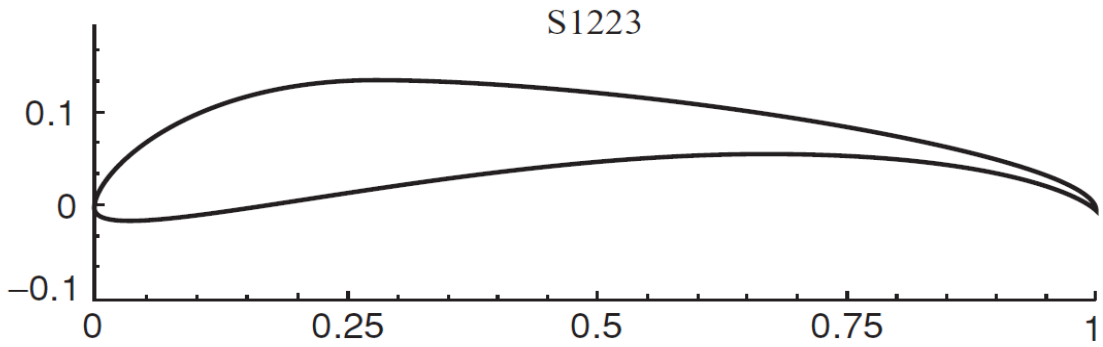

Figure 1 Airfoil Selection

Table 2 Airfoil parameters

Area	0.06614
Thick	0.12124
camber	0.08894
Rad_{LE}	0.04450
$\Delta\theta_{TE}$	67.68°

3.1.2.1 wing planform

The wing is most second important piece in the aircraft design after airfoil selection so there must be very careful in choosing wing area, chord, sweep angle and location that is must produce the required lift.

Taking into account the design specification wing planform have been chosen like seagull wing in dimension, size, and shape which closely meets our design specification the wing dimension were chosen in such way that they produce enough lift to keep the model in air with forward velocity 5 m/s and flapping frequency 3 HZ that is min velocity and max frequency.

Table 3 Wing dimension

Wing area	0.628 m2
Wing span	2 m
Mean aerodynamic chord	0.336 m
Airfoil	S1223

3.1.2.2 model and reference geometry

The fuselage was designed in such way that it has enough space to hold the mechanism and flight system in simple way with no interference and produce low drag and it has low negative contribution to overall stability and look like same as seagull.

Finally, a horizontal stabilizer or tail was designed and it was sized in way that it controls the stability of the model in flapping and gilding flight and it allow for all the tail to move as one part. The dimension taken from the seagull configuration

Table 4 Model Geometry

Tail area	0.174 m2
Tail mean aerodynamic chord	0.444m
Fuselage max diameter	0.2 m
Fuselage length	1.0 m
Fuselage area	0.132 m2
Tail airfoil	NACA 0012

3.1.2.3 wing kinematics

Birds or flapping wing flyers has complex pattern which involve translation and rotation motion with several degrees of freedom and even deformation. In our case and for simplicity we represent the flapping motion as the roll motion about X axis with wing has two parts as internal and external wing and the internal wing flap about reference X axis (1,0,0) and external wing flap about internal wing axis so external wing flapping axis depend on internal wing location. And the equation that describe the motion are as follows:

$$roll_{iw} = A_{iw} * \sin(w * t) \quad \text{(1)}$$

$$droll_{iw} = A_{iw} * w * \cos(w * t) \quad \text{(2)}$$

$$roll_{ew} = -\frac{A_{ie} * {}^{\pi}/_{2} * \text{erf}(\sqrt{2} * \sqrt{B} * \cos(\omega * t))}{2 * \sqrt{B} * C} \quad \text{(3)}$$

$$droll_{ew} = \frac{A_{ie} * w * \sin(w * t) * e^{(B * \sin\left(2 * w * t - \frac{\pi}{2}\right) - B)}}{C} \quad \text{(4)}$$

Where:

roll is the roll angle of the wing in degree

droll is the angular velocity in degree/second

the subscript (iw) stands for internal wing, the subscript (ew) stands for external wing,

A_{iw} is the maximum roll amplitude of the internal wing, A_{ie} is the maximum angle between the internal wing and external wing,

W: is the angular frequency ($2\pi f$), f is the flapping frequency,

t : is the time

and erf is the error function

the amplitude A_{iw} is equal to 30 degrees the amplitude A_{ie} is equal to 50 degrees

B and C are constant B=1 and C = 1.1963

The kinematic was designed in such way that it produces the required lift and thrust at design condition of forward velocity 5 m/s and flapping frequency 3 HZ this equation produce flapping motion close to the actual birds.

3.1.3 Aerodynamic analysis

Aerodynamic analysis of flapping wing is the top challenge in aerodynamic analysis because it is unsteady aerodynamic and low Re number and also there is not enough information about it and the flow behavior at low Re is very different from that in high Re number because in low Re the flow has low energy and the boundary layer has strong effect and it is difficult to perform the analysis in computational way because all commercial software designed for fixed wing analysis so, there must be lot of change in the program and use advance setting to do the analysis and that means complete knowledge of the program and analytically is more difficult that in the flapping wing there is two main components of velocity forward, component due to flapping motion, and induced velocity, so the effective free stream velocity change along the span and that lead to change in angle of attack along the span.

Also, vortex generation in leading edge due to flapping motion and the wake of wing has strong effect in lift generation. All these lead to complex equation to calculate lift distribution along the span.

3.1.3.1 CFD analysis

In the analysis the unsteady incompressible Reynolds-Averaged Naiver –Stokes equation are solved by using the commercial finite volume solver Ansys fluent (16). The cell-centered value of the computed variable is interpolated at the face location using second-order centered difference scheme for the diffusion terms. the convective terms at cell at cell faces are interpolated by means of second –order upwind scheme. For computing

the gradients at cell –centers, the least squares cell-based reconstruction method is used. In order to prevent spurious oscillations a multidimensional slope limiter is use which enforce the monotonicity principle by prohibiting the linearly reconstructed filed variables on the cell faces to exceed the maximum or minimum of the neighboring cells. This result in total variation diminishing(TVD) scheme that guarantees the accuracy.

Stability and boundedness of the solution. The pressure-velocity coupling is achieved by means of the PIZO algorithm and as the solution takes place in collected meshes, the Rhie-Chow interpolation scheme is used to prevent the pressure checkerboard instability. For turbulence modeling, the Shear Stress Transport (SST) $\boldsymbol{k\omega}$ model is used with wall function and low Re correction. The turbulence quantities, turbulent kinetic energy k and specific dissipation rate $\boldsymbol{\omega}$, are discretized using the same scheme as for the convective terms. To handle the moving bodies, the dynamic meshing model was employed where we use mesh diffusion layering and Re-meshing was used every time-step. The lift force, drag and thrust are calculate by integrating the pressure and shear stress over surface of the model and then CL and CD are computed.

3.1.3.2 Dynamic mesh

In the aerodynamic analysis of flapping wing the most important and complex part is the dynamic mesh. Dynamic mesh deals with domains of fluid which has boundary change with time. The wing of the model moving with time and so the domain and that lead to change in the meh of any tiny element in time so the element size change with time. For all this reason the mesh quality and time step size have to be adjusted carefully to avoid the dynamic mesh problem like negative element volume.

3.1.3.3 User define function (UDF)

The UDF's is programming code which control the motion of moving part of the surface. They usually writing in C language and they need some reference point into the mesh. For this reason, all the reference systems of the CAD drawing, the solid model and the mesh have to match on the same point. In our model the UDF that we use to describe the motion is consisting of two part UDF for internal wing and UDF for external wing and every one with different equations of motion as that describe above in wing kinematics and we need more equation than the equation in wing kinematic to define the external wing motion and this equation are in the appendix.

The UDF code for internal wing motion are as in appendix A.

3.1.3.4 Mesh setting

For all above reasons the mesh setting and the quality are important and the quality must be high as possible for this the domain size and shape and the element size and number must be carefully determined. The element number also effect the solution process and the time of solution with this the skewness of the mesh has strong effect also. The domain was made big enough to contain the model and the motion in a way that the motion of mesh did not make any negative volume and no interaction between the body and the boundary condition or walls with volume 25 m3. The number of element and size were adjusted in

such a way that the elements have high concentration near the model and has low concentration far from the model or near the walls with element number 357412 and the max skewness was 0.91721 the mesh has done.

Table 5 Fluent mesh sizing

Domain dimension	(25000*25000*25000) mm
Mesh type	Unstructured dynamic mesh
Nodes number	62067
Element number	357412
Skewness	0.91721
Face sizing for domain:	
Geometry	6 faces
Suppressed	No
Type	Element size
Element size	300mm
Behavior	Hard
Face sizing for model	
Geometry	37 faces
Suppressed	No
Type	Element size
Element size	25mm

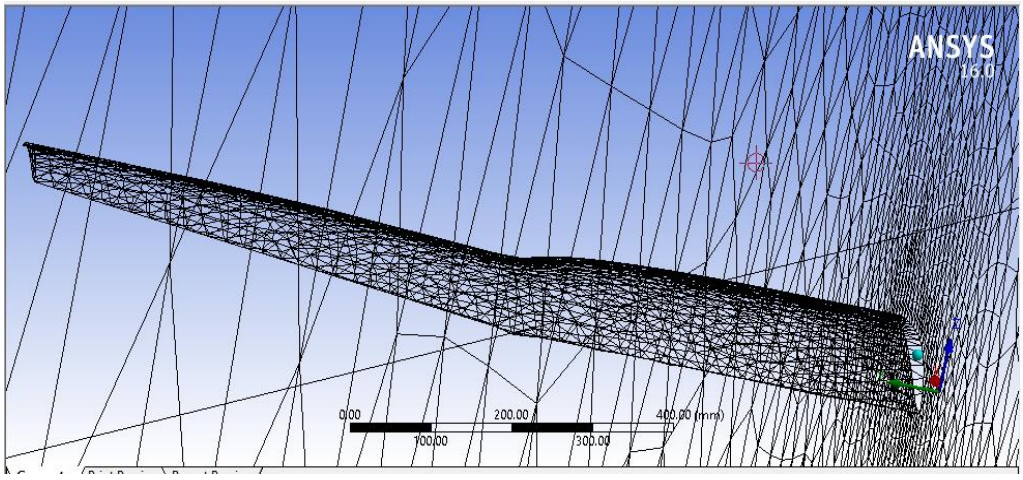

Figure 2 Wing mesh

3.1.3.5 Fluent Setting

Table 6 Fluent setting

Setup	Adjustments
General	
Type	presser-based
Time	transient
Model	k-omega SST
Materials	Air
Cell zone conditions	Fluid
Boundary condition	
Inlet	
Outlet	Pressure-outlet
Dynamic mesh	Smoothing, layering, re-meshing.
Reference value	
Area	0. 628
Length	0.336
Solution methods	
Scheme	PIZO
Skewness correction	0
Pressur	Second order
Momentum	Second order upwind
Run calculation	
Time setup size	0.0001 s
Number of time setup	3333

3.1.4 Analytical analysis

Analytical analysis for aerodynamics of flapping wing is big challenge for all aerodynamicist and to have good result or high accuracy is more challenging because it deals with low Re and unsteady aerodynamic and has complex flow motion you have forward and flapping motions. In the analysis used analytical analysis with some simplification to have result close to the real one. The equation and method that was used are come from handbook “How Ornithopters Fly” in German only. These equations calculate the forces of flapping wing used quasi-steady numeric wing stripes method it is good enough in case of fast forward flight with relatively low flapping frequency like large bird in cruise flight and this is close to our model.

The equation used to calculate the aerodonetic characteristic are as follow:

3.1.4.1 At gliding condition

Gliding velocity:

$$V_G = \sqrt{\frac{2m_M * g}{\rho * I_m * b * c_{amG}}} \text{ ……..……..... (5)}$$

Average circulation:

$$\Gamma_{mG} = \frac{m_M * g}{\rho * V_G * b} \text{…….……..…….... (6)}$$

Aerodynamic center distance to the wing root in relative to (b/2) semi-span:

$$y_{rG} = \frac{C_{rG}}{6 * \pi} \text{…….……...…….....…….... (7)}$$

In order to use the lifting line theory, there is a need to calculate the circulation distribution on the wing span by the following eq.:

Circulation is:

$$\Gamma_{G(y)} = \Gamma_{mG} * \left[\left(\frac{12}{\pi} - 6y_{\Gamma G} \right) * \sqrt{1 - \left(\frac{y}{s}\right)^2} + \left(18y_{\Gamma G} - \frac{24}{\pi} \right) \left(\frac{y}{s}\right)^2 * arccosh * \left(\frac{s}{y}\right) \right] \text{... (8)}$$

Lift coefficient:

$$C_{aG(y)} = \frac{2 * \Gamma_{G(y)}}{I * V_G} \text{…….……..…….... (9)}$$

Angle of attack distribution along the span:

$$\alpha_{G(y)} = \alpha_0 + \frac{C_{aG(y)}}{C_\alpha} \text{…….……..…….....……... (10)}$$

Induced velocity (Upwind):

$$V_{iG(y)} = \Gamma_{mG} * \frac{9}{s} * \left[\frac{1}{\pi} - \frac{2}{3} * y_{\Gamma G} + \left(\frac{\pi}{2} * y_{\Gamma G} - \frac{2}{3}\right) * \frac{y}{s}\right] \ldots\ldots\ldots\ldots \quad (11)$$

Angle of induced velocity:

$$\alpha_{iG(y)} = arctan \frac{V_{iG(y)}}{V_G} \ldots\ldots\ldots\ldots\ldots\ldots\ldots\ldots \quad (12)$$

Angle of incidence distribution at the wing.

$$\alpha_{EG(y)} = \delta_{G(y)} + \alpha_{G(y)} + \alpha_{iG(y)} - \sigma \ldots\ldots\ldots\ldots\ldots\ldots\ldots \quad (13)$$

3.1.4.2 Powered flight in general

Maximum angular velocity for both clocks lt. Eq. 5.5, with φE in degrees

$$\omega_{max} = \pm \frac{\pi^2 * \phi_E}{90 * t_p} \ldots\ldots\ldots\ldots\ldots\ldots\ldots\ldots\ldots\ldots \quad (14)$$

Airspeed in powered flight (speed at flapping condition).

$$V_k = V_G * K_V \ldots\ldots\ldots\ldots\ldots\ldots\ldots\ldots\ldots \quad (15)$$

3.1.4.3 Upstroke

Resultant aerodynamic force location:

Aerodynamic center distance to the wing root in relative to (b/2) semi-span:

$$y_{\Gamma 1} = \frac{C_{\Gamma 1}}{6 * \pi} \quad \ldots\ldots\ldots\ldots\ldots\ldots\ldots\ldots\ldots\ldots\ldots\ldots\ldots\ldots\ldots\ldots \text{(16)}$$

Circulation factor:

$$k_{\Gamma} = \frac{\frac{2-\pi * y_{\Gamma G}}{I_{(0)} * C_{\alpha}} + \frac{270}{b} * \left(\frac{1}{\pi} - \frac{2}{3} * y_{\Gamma G}\right)}{\frac{2-\pi * y_{\Gamma 1}}{I_{(0)} * C_{\alpha}} + \frac{270}{b} * \left(\frac{1}{\pi} - \frac{2}{3} * y_{\Gamma 1}\right)} \ldots\ldots\ldots\ldots\ldots\ldots\ldots\ldots\ldots\ldots\ldots \text{(17)}$$

average circulation:

$$\Gamma_{m1} = \Gamma_{mG} * k_{\Gamma} \ldots\ldots\ldots\ldots\ldots\ldots\ldots\ldots\ldots\ldots\ldots\ldots\ldots\ldots\ldots \text{(18)}$$

In order to use the lifting line theory, there is a need to calculate the circulation distribution on the wing span by the following eq.:

Circulation is:

$$\Gamma_{1(y)} = \Gamma_{mG} * \left[\left(\frac{12}{\pi} - 6y_{\Gamma 1} \right) * \sqrt{1 - \left(\frac{y}{s}\right)^2} + \left(18y_{\Gamma 1} - \frac{24}{\pi} \right) \left(\frac{y}{s}\right)^2 * arccosh * \left(\frac{s}{y}\right) \right] \ldots \text{(19)}$$

Vertical speed due to flapping motion:

$$V_{u1(y)} = s * \frac{y}{s} * \omega_{max} \ldots\ldots\ldots\ldots\ldots\ldots\ldots\ldots\ldots\ldots\ldots\ldots\ldots\ldots\ldots\ldots\ldots\ldots\ldots\ldots \text{(20)}$$

Effective free stream velocity:

$$V_{e1(y)} = \sqrt{{V_{u1(y)}}^2 + {V_K}^2} \quad \text{..... (21)}$$

Lift coefficient:

$$C_{a1(y)} = \frac{2*\Gamma_{1(y)}}{I*V_{e1(y)}} \quad \text{..... (22)}$$

Angle of attack distribution along the span:

$$\alpha_{1(y)} = \alpha_0 + \frac{C_{a1(y)}}{C_\alpha} \quad \text{..... (22)}$$

Induced velocity (upwind)

$$V_{i1(y)} = \Gamma_{m1} * \frac{9}{s} * \left[\frac{1}{\pi} - \frac{2}{3} * y_{\Gamma 1} + \left(\frac{\pi}{2} * y_{\Gamma 1} - \frac{2}{3}\right) * \frac{y}{s}\right] \quad \text{..... (23)}$$

Angle of induced velocity:

$$\alpha_{i1(y)} = \ arctan \frac{V_{i1(y)}}{V_{e1(y)}} \quad \text{..... (24)}$$

Incidence angle:

$$\delta_{1(y)} = \ arctan \frac{V_{u1(y)}}{V_k} \quad \text{..... (25)}$$

Angle of incidence distribution at the wing.

$$\alpha_{E1(y)} = \delta_{1(y)} + \alpha_{1(y)} + \alpha_{i1(y)} - \sigma \quad \text{..... (26)}$$

wing twisting characteristic

$$V_{\Delta\alpha 1} = \frac{2*(\alpha_{E1(y)} - \alpha_{EG(y)})}{S} \quad \text{..... (27)}$$

3.1.4.4 Down stroke

Resultant aerodynamic force location:

Aerodynamic center distance to the wing root in relative to (b/2) semi-span:

$$y_{r2} = \frac{C_{r2}}{6*\pi} \quad \text{..... (28)}$$

Circulation factor:

$$k_{\Gamma 2} = \frac{\frac{2-\pi*y_{\Gamma G}}{l_{(0)}*C_\alpha} + \frac{270}{b}*\left(\frac{1}{\pi} - \frac{2}{3}*y_{\Gamma G}\right)}{\frac{2-\pi*y_{\Gamma 2}}{l_{(0)}*C_\alpha} + \frac{270}{b}*\left(\frac{1}{\pi} - \frac{2}{3}*y_{\Gamma 2}\right)} \quad \text{..... (29)}$$

Average circulation:

$$\Gamma_{m2} = \Gamma_{mG} * k_{\Gamma 2} \quad \text{..... (30)}$$

In order to use the lifting line theory, there is a need to calculate the circulation distribution on the wing span by the following eq:

circulation

$$\Gamma_{2(y)} = \Gamma_{mG} * \left[\left(\frac{12}{\pi} - 6y_{\Gamma 2}\right) * \sqrt{1 - \left(\frac{y}{s}\right)^2} + \left(18y_{\Gamma 2} - \frac{24}{\pi}\right)\left(\frac{y}{s}\right)^2 * arccosh * \left(\frac{s}{y}\right)\right] \text{... (31)}$$

Vertical speed due to flapping motion:

$$V_{u2(y)} = s * \frac{y}{s} * \omega_{max} \quad \text{..... (32)}$$

Effective free stream velocity:

$$V_{e2(y)} = \sqrt{{V_{u2(y)}}^2 + {V_K}^2} \quad \text{..... (33)}$$

Lift coefficient:

$$C_{a2(y)} = \frac{2*\Gamma_{1(y)}}{I*V_{e2(y)}} \quad \text{..... (34)}$$

Angle of attack distribution along the span:

$$\alpha_{2(y)} = \alpha_0 + \frac{C_{a2(y)}}{C_\alpha} \quad \text{..... (35)}$$

Induced velocity (Upwind):

$$V_{i2(y)} = \Gamma_{m2} * \frac{9}{s} * \left[\frac{1}{\pi} - \frac{2}{3} * y_{\Gamma 2} + \left(\frac{\pi}{2} * y_{\Gamma 2} - \frac{2}{3}\right) * \frac{y}{s}\right] \quad \text{..... (36)}$$

Angle of induced velocity:

$$\alpha_{i2(y)} = \ arctan \frac{V_{i2(y)}}{V_{e2(y)}} \quad \text{..... (37)}$$

Incidence angle:

$$\delta_{2(y)} = \ arctan \frac{V_{u2(y)}}{V_k} \quad \text{..... (38)}$$

Angle of incidence distribution at the wing.

$$\alpha_{E2(y)} = \delta_{2(y)} + \alpha_{2(y)} + \alpha_{i2(y)} - \sigma \quad \text{..... (39)}$$

3.2 Structure

3.2.1 **3.2.1 Material selection**

This aircraft should be much lighter and should withstand much higher loads which mean the materials that will use to fabricate it must be have specific strength and specific stiffness. Obviously these properties are better in the composite materials than in metals, in addition the composite materials can be machined, formed and repaired much easily as compared to the conventional metallic structures.

When selecting composite material for manufacturing, the following points should be taken in account:

- Cost
- Commercial availability
- Multiple material source
- Easy of processing, Manufacturing, and handing
- Ability to be used in automated manufacturing process

According to above points, the carbon fiber woven 395 GPa is selected for manufacturing the wing spars although it is very expensive, but it is the most suitable option for the spars that subjected to high loads. The fiberglass type S is selected to manufacturing the all other structural components, because it is low cost, low weight, and has good strength.

Vacuum Assisted Resin Transfer Molding (VARTM) method, was selected to manufacture the aircraft. In this production technique, the woven fibers previously mixed with resin (pre-preg). The vacuum forming technique has many advantages include: The exact shape of the model can be made easily and it is not a very time-consuming process. In addition, the manual handwork can be used to fabricate the LAV. Therefore, the fabrication cost can be reduced.

However, this method has a few disadvantages:

- Toxic gases will be released if the heating is exceeding.
- Non-uniform wall thickness will occur during stretching process.

Also the (VARTM) fabrication method is very sensitive to environmental conditions; the temperature and pressure of the manufacturing environment is the main parameter that

determine the final product strength. Depending on the material used, fabricating at temperatures higher than atmospheric temperature make the viscosity decreasing resulting in homogenous matrix, so the structure become stronger

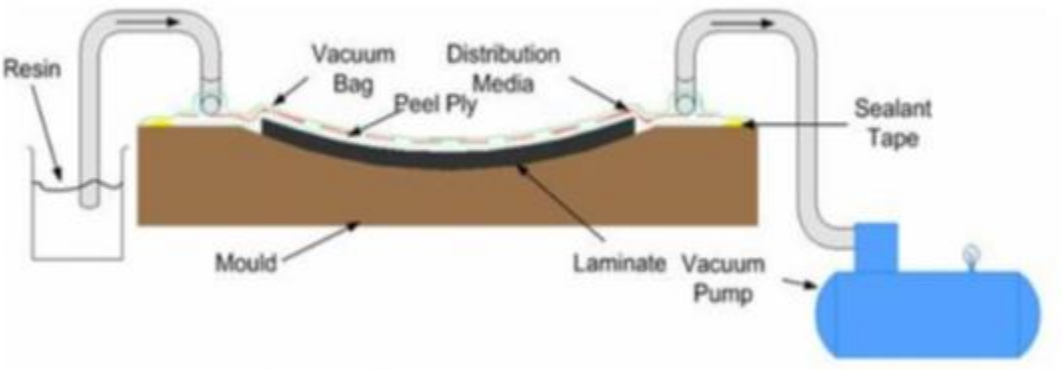

Schematic representation of VARTM process

3.2.2 **CATIA Drawing**

Aircraft configuration:

The case study was selected to be the sea-gull because it has good aerodynamic characteristics and relatively simple configuration compared with other birds. The dimension and whole configuration were derived from old researches for simplification and accuracy. All drawing was done by using catia software.

3.2.2.1 Wing

Our case study's wing is divided into two parts: inner wing and outer wing with angle of 25^{o} between them and the internal structure was drawn as follows:

3.2.2.1.1 Ribs

The ribs were made by importing the selected airfoil (Selig 1223) using excel and then distribute them along the wing with certain distance between the according to load distribution "based on precedent researches" and then give each airfoil a pad of 1mm to get the conventional shape of the rib shown below:

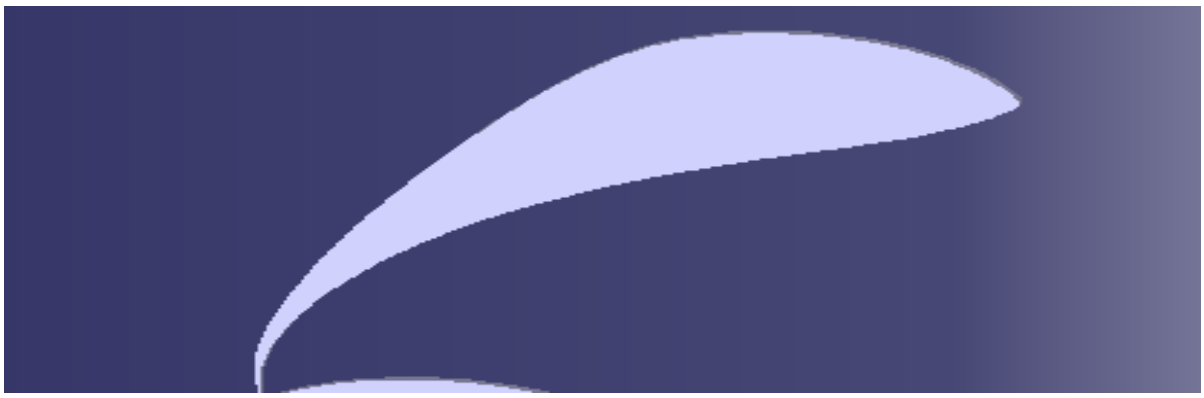

Figure 3 Rib

3.2.2.1.2 Spar

The function of this part is to transfer the load subjected on the wing to the fuselage. First we holed each rip along span at quarter chord and create a cylindrical hollower spar with diameter of 15mm- due to loading and thickness limitation of each aerofoil- passing through these holes using removed-multi section icon in CATIA software.

Since it has a little small diameter, and while it has to transfer the load from the wing, this spar must be made from slight and strong material such as carbon fiber to resist deformation and failure. Spar final shape is shown below:

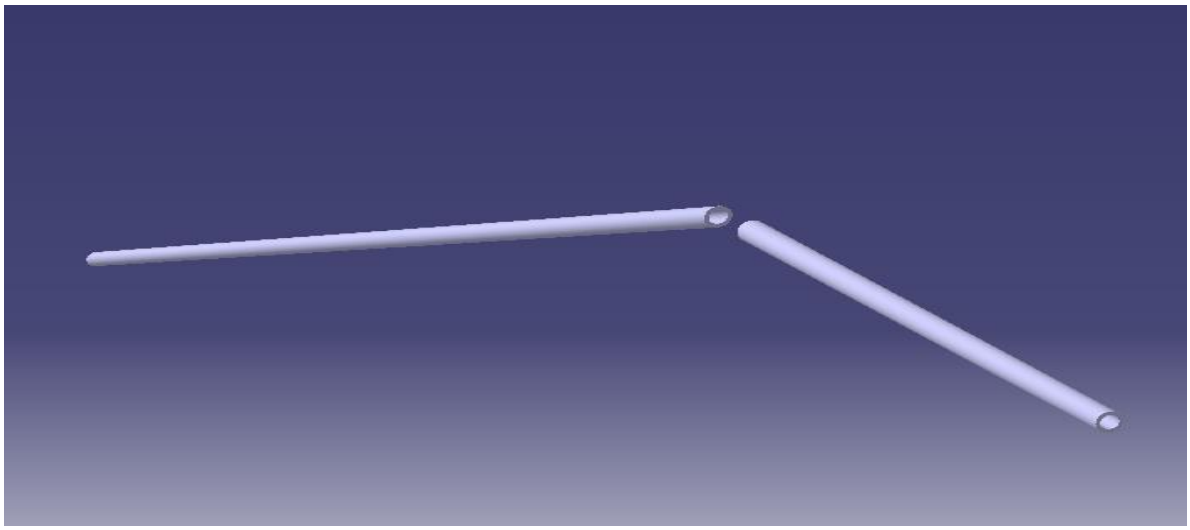

Figure 4 Spar

3.2.2.1.3 Stringer

The same procedure to draw the spar was done to draw stringer except that the stringer's diameter is 10mm and it passes through leading edge point of each rip.

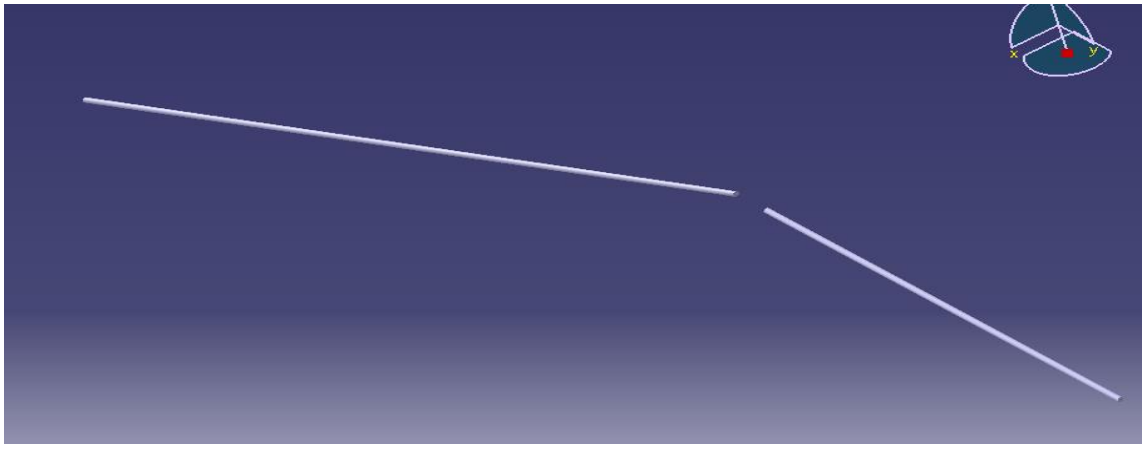

Figure 5 Stringer

All these parts were covered by a skin of 0.3mm to give the wing its conventional shape shown below:

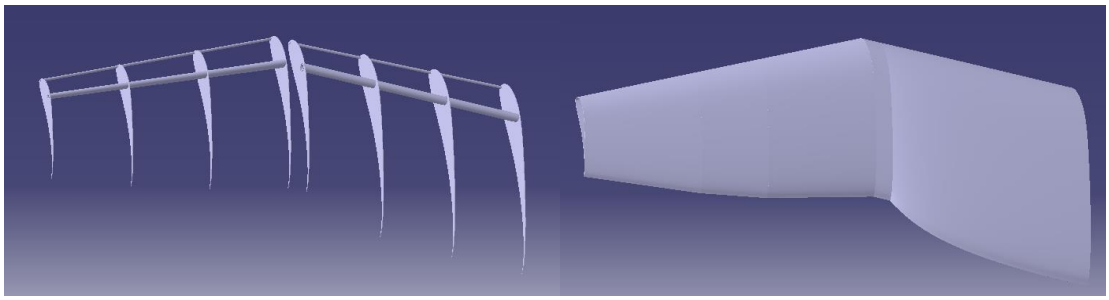

Figure 6 Wing internal structure

3.2.2.2 Fuselage

To draw the fuselage, we had first to draw the top and side view of the model and then draw the frames sketches from the interaction of these two views and then give these frames a pad of 1mm in order to handle with the load transferred from the wing, preventing fuselage from being damaged. Finally cover these frames with skin of 0.3mm.

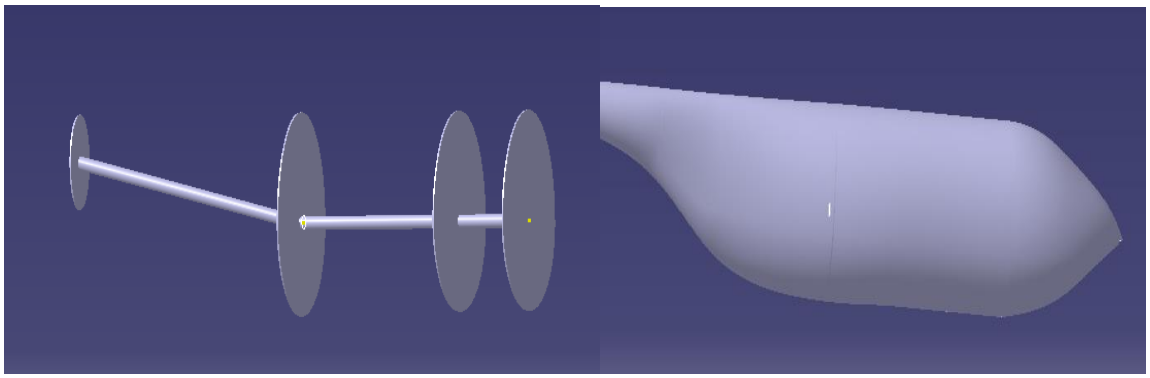

Figure 7 Fuselage

3.2.2.3 Tail

Just like wing we imported tip and root airfoils of the tail using excel and then draw the configuration of the tail by connecting these airfoils by spline and give this shape a thickness of 0.3mm.

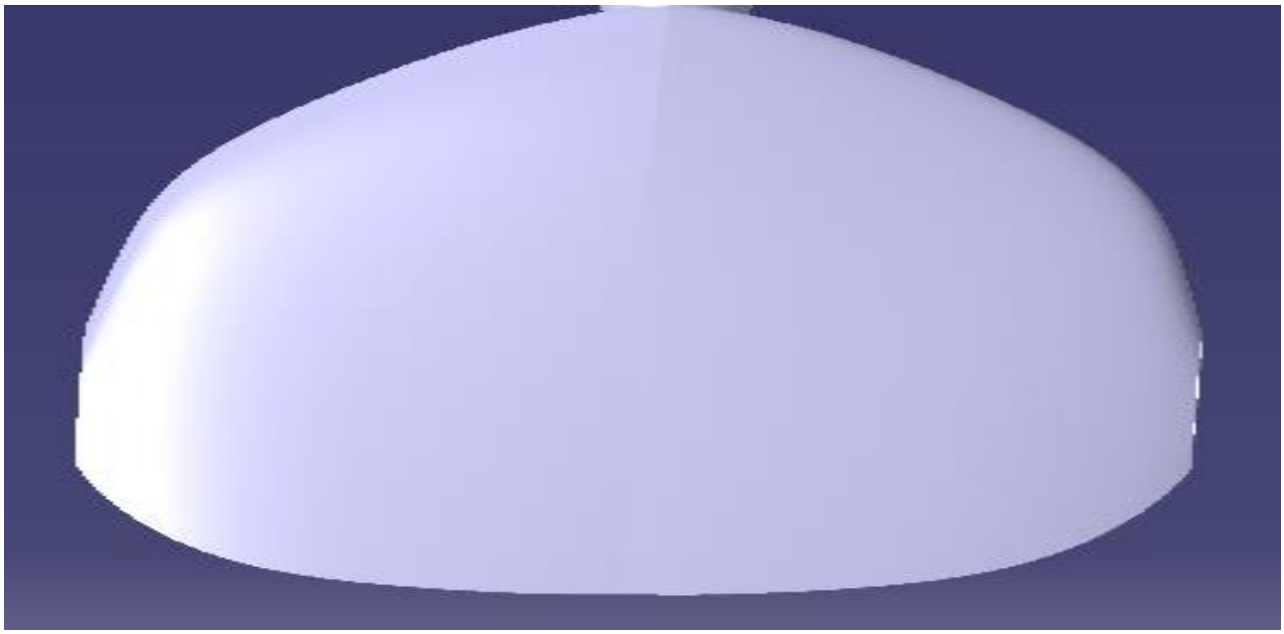

Figure 8 Tail

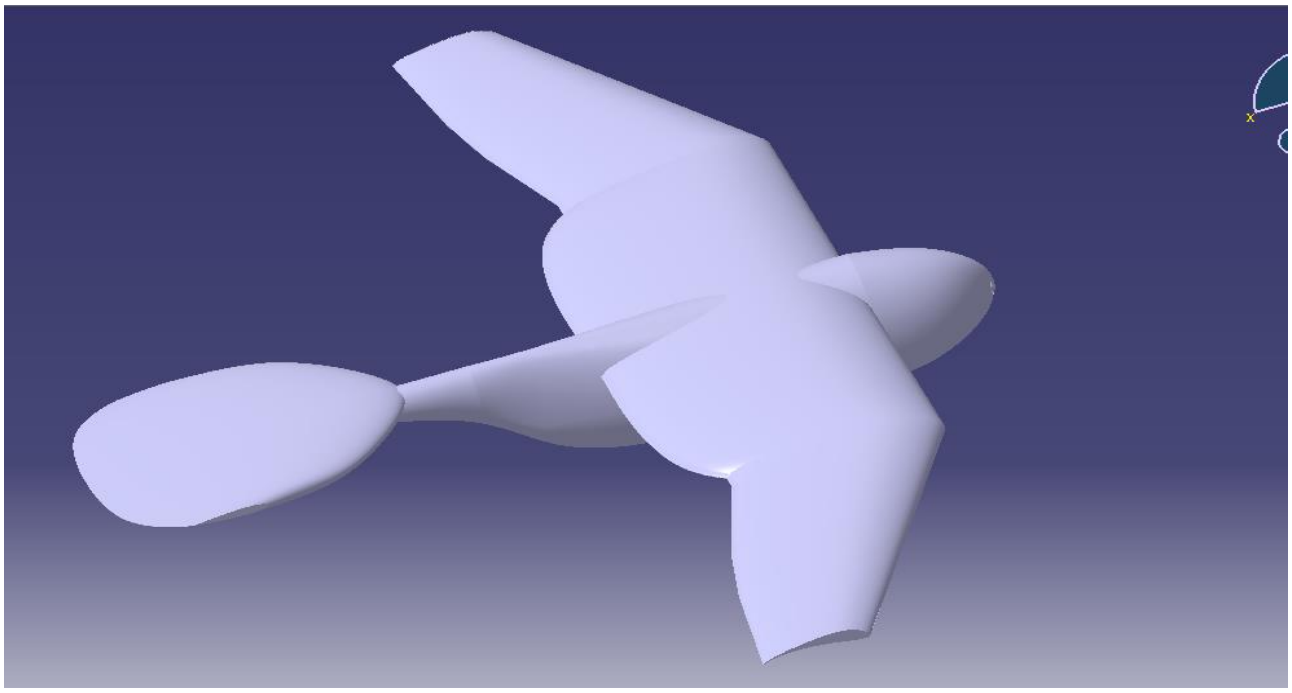

Figure 9 Complete model

3.2.3 Weight Estimation

from table (1), the model's weight is 9.81 (N), we estimated the weight of each component of the structure.

Every components volume was estimated using CATIA software and then multiply it by the density of the components material to obtain the components mass.

The weight of each component of the structure is in table (7).

Table 7 Structure weight

Component	Weight (N)
Wing	
External spar	0.5
Internal spar	0.5477
Rips	0.844
External stringer	0.124
Internal stringer	0.124
Total wing	2.1397
For 2 wings	4.2794
Fuselage	
Frames	2.258
Spar	0.21
Total fuselage weight	2.468
Tail	
Tail	1.2
System	
Battery	0.8632
Motor	0.5297
Total system weight	1.3929
Mechanism	
The two gears	0.6626
Rod (B)	1.06626
Rod (A)	0.05929
Connection at point (2)	0.25146
Connection at point (5)	0.1937
Total mechanism weight	2.23331
Total structure weight	9.8

3.2.4 Structure Analysis

The internal structural components of the wing have been analyzed using ANSYS, Linear structure analysis to estimate the deformation.

3.2.4.1 Geometry

It is known -in flapping wing- that the fuselage and tail are not essential surfaces in creating lift and thrust, the only function of the tail is for control. Hence our geometry to be tested is only the wing as it is the main surface which is subjected to the loads and has to deal with these loads.

3.2.4.2 Mesh

Meshing process -as mentioned in aerodynamic section- is the most important process in the analysis because the result accuracy depends on mesh type and sizing.

In our case -flapping wing-, there is not a standard mesh sizing that can be executed to lead to logical results, so we had -after knowing the meaning of each mesh -, we had to use try and error method until we reach the suitable sizing.

Table 8 Mesh sizing for structure analysis

Sizing	
Use advanced size function	On: curvature
Relevance center	Coarse
Initial size seed	Active assembly
Smoothing	Medium
Transition	Low
Span angle center	Fine
Curvature normal angle	15°
Minimum size	0.476720 mm
Maximum face size	60 mm
Maximum size	95.3440mm
Growth rate	1.20
Minimum edge length	6.9018*e^-0.003 mm
Statistics	
Nodes	299452
Element	58150
Mesh metric	Skewness
Minimum	1.5087*e^-0.002
Maximum	0.88809
Average	0.36776
Standard deviation	0.17571

3.3 Mechanism concept

Natural flyers have amazing mechanism to create lift and thrust by moving the wings in the three axes (pitching, flapping, lagging). But it is very difficult to simulate this mechanism because of high stress and moments will be applied on the structure. and due to this reasons we simulate the only flapping motion.

The propose here is transmit the rotational motion of DC motor to the components of the mechanism system and convert this rotational motion to linear motion to get exact movement of wings as required from aerodynamic analysis.

This converting process start with two gears dovetailed together and every gear has small shaft fixed in the point on the cross section of the gear, and this point is chosen respect to the angle required to the internal spar and those two gears must be fixed on the bulkhead of the fuselage, and inside the fuselage as shown in the figure (10).

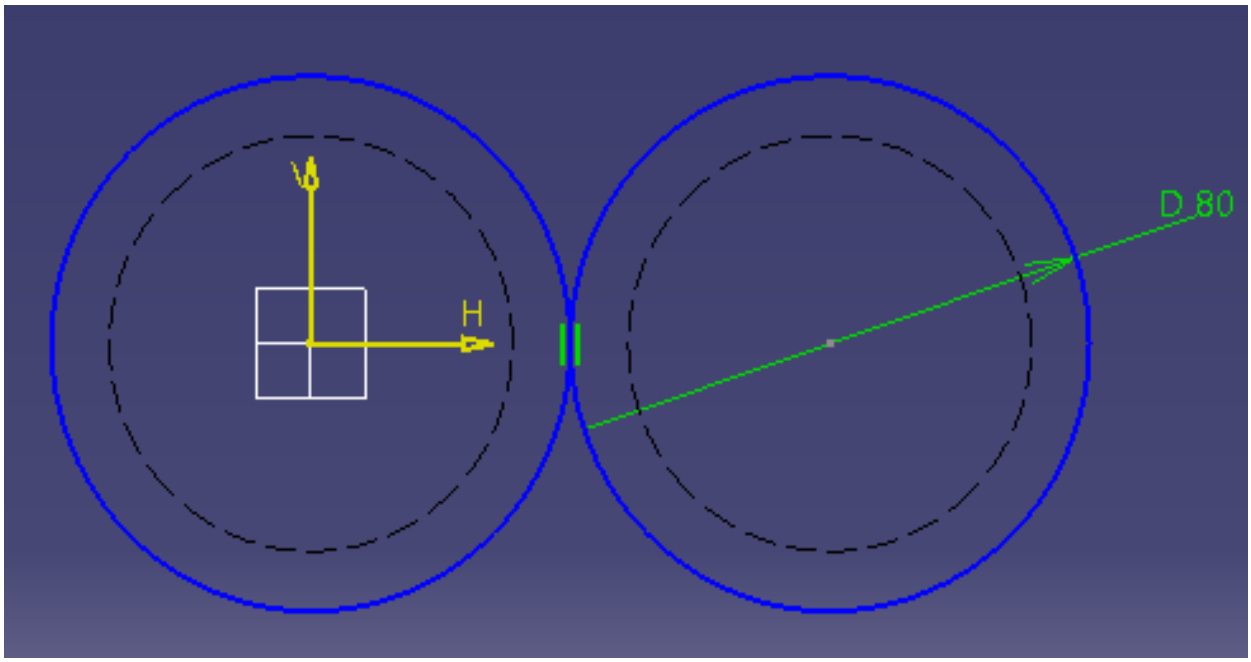

Figure 10 Gears 2D view

The internal spar also fixed in the bulkhead parallel to the gears latterly, and the rod (A) is connected to the internal spar in the point (2) and the other end is connected with the gear by small shaft discussed previous at point (1), when the gears start rotating, the rod (A) will move up and down, and with the movement of rod (A) the internal spar will move, therefore, we get the flapping movement in the internal spar, thus, internal wing as shown in the figure (11).

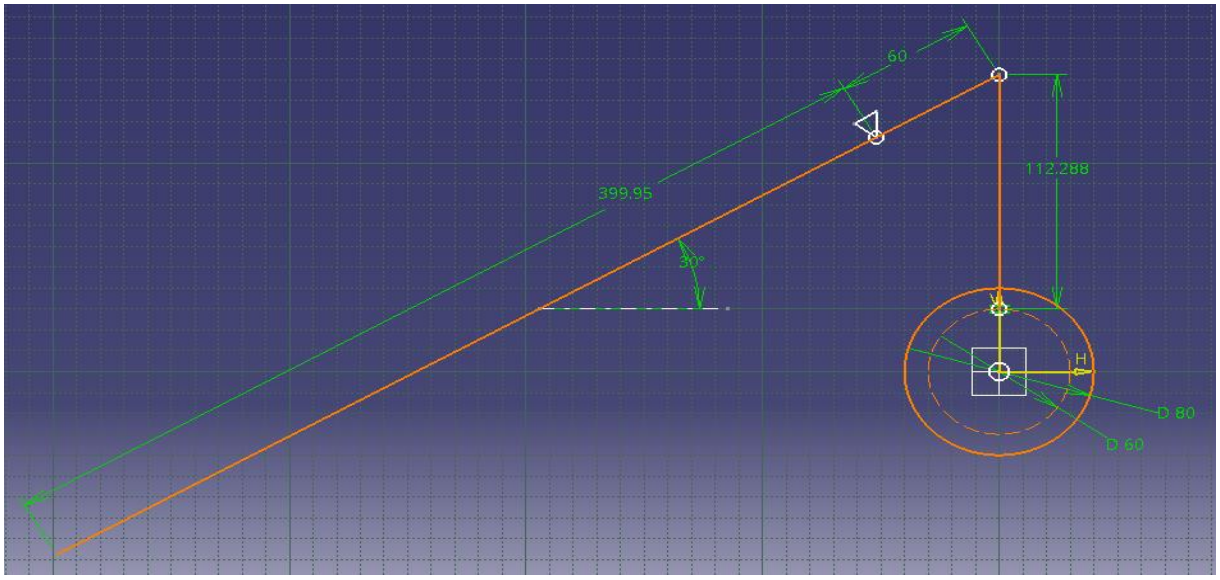

Figure 11 Internal wing connection

NOW, how the external wing work?

Figure (12) illustrate the complicated components of the mechanism motion firstly, internal and external spars and rod (A), rod (B) and gears, the connection of rod (A) is discussed previous, rod (B) is connected to the rod (A) at point far from point (2) by vertical distance available inside the wing and the other end of rod (B) is connected to the external spar and the outer end of the internal spar is connected to the internal end of the external spar.

When the gear starts rotating, rod (A) will move up and down as discussed previous and rod (B) will move left and right parallel to the (IS) due to change in angle of rod (A) then the rod (B) will change the angel of external spar then external wing.

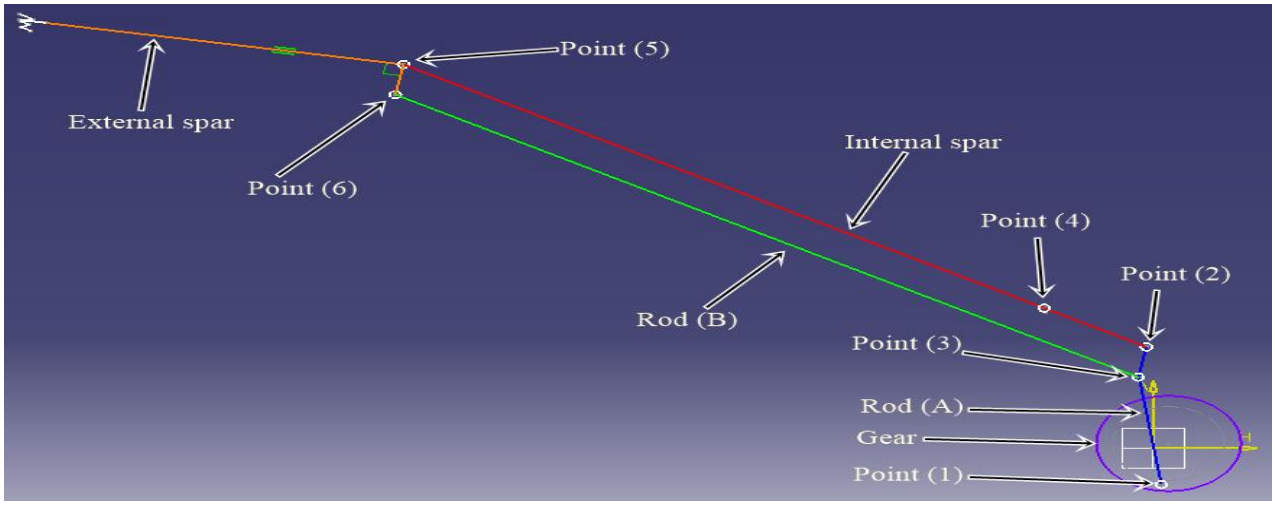

Figure 12 Mechanism components and connection points

The question asked here is how the required angels for internal and external spares can be achieved?

3.3.1 Mathematic expression

Firstly, the diameter (D) of the two gears must be specified to be as big as possible and it is limited by the space available inside the fuselage, then, specifying the length of internal spar inside the fuselage (Li) as big as possible to reduce the moment required from dc motor with take in account the vertical space required to this length when it is move up and down, finally the angels for internal and external spars have been already obtained from aerodynamic analysis and the (D), (Li), (d) and (IS), (ES) is also obtained . All these parameters are shown in table (9).

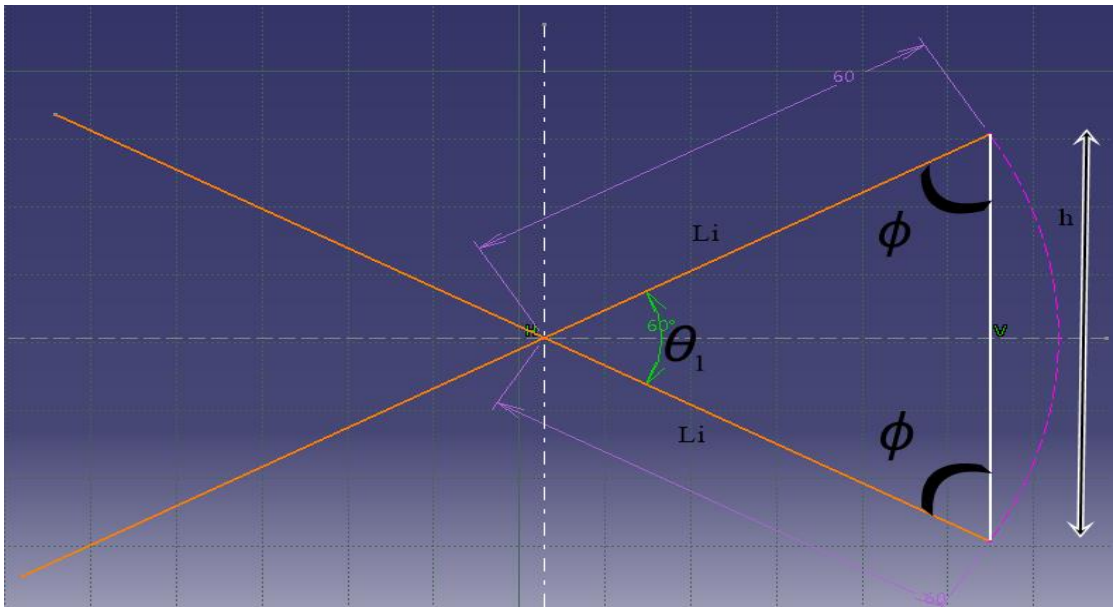

Figure 13 Vertical distance of internal spar inside fuselage

From figure (13)

$$\frac{sin\theta_1}{h} = \frac{sin\phi}{L_i} = \frac{sin\phi}{L_i}$$

$$\phi = \frac{180 - \theta_1}{2}$$

$$\frac{sin\theta_1}{h} = \frac{\sin(\frac{180 - \theta_1}{2})}{L_i}$$

$$\boldsymbol{h} = \frac{L_i sin\theta_1}{\sin(\frac{180 - \theta_1}{2})}$$

Then the dimeter of the connection at gear must be equal (h) to get the distance required as shown in figure (14).

$$h = d = \frac{6 * sin30}{\sin(\frac{180 - 30}{2})} = 3.10583cm$$

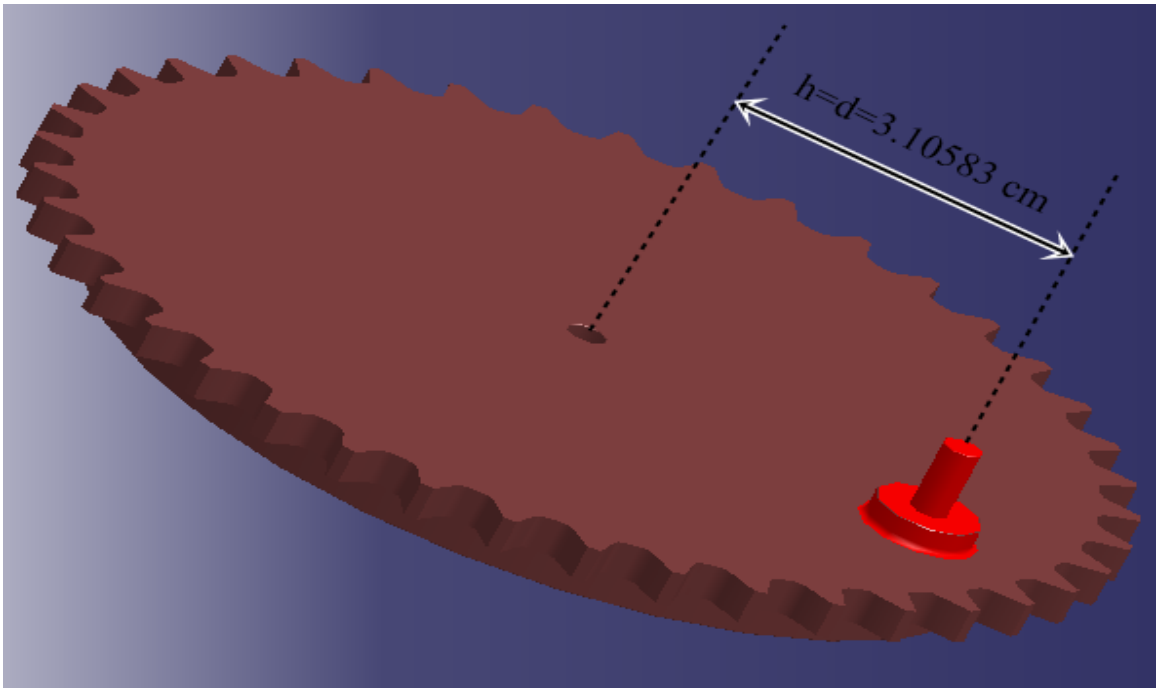

Figure 14 Position of point 1 on the gear

3.3.2 **external wing calculation**

According to this configuration, the external wing will have inclined with the same angle of the rod (A) during rotation of the gears and we can adjust this angle by changing distance ratio between points (2-3) and points (5-6) -as shown in fig 3- , but in this case there is no need to adjust this angle because the required angle is 60 degree and rod (A)

will inclined 30 degrees every cycle, and internal spar also have inclination 30 degree every cycle then the sum equal 60 degrees.

Figure 15 Inclination angle of distance between points (2-3) with the other length of rod

But with this shape of rod (A) as show in figure (14) the external spar will have upward incline at neutral position, to solve this problem, the distance from points (2-3) must be inclined by angle (15) degree with the other length of rod (A) as shown in figure (15).

Table 9 Parameters value

parameter	value
θ_1	30̊
θ_2	60̊
L_i	6 cm
IS	38.33 cm
ES	58.33 cm
Rod (A)	11.59 cm
Rod (B)	38.33 cm
Distance from points (2-3)	2.5 cm
Distance from points (5-6)	2.5 cm

3.4 System selection

3.4.1 Power calculating

The power estimation is depending on the specification of the similar flapping wing aircrafts based on comparison of the power to weight ratio. The FESTO UAV "SmartBird" specifications can be considered as a baseline for our calculation, it weighs 0.45 kg and its motor power is 23 W, so the power to weight ratio equal to 51.111 W/kg. When apply this in our aircraft of weight 1 Kg, the power required from the motor will equal to 51.111 W.

This result is very accurate due the two aircraft is similar in shape, type of material used and the internal structure configuration.

3.4.2 Motor and Battery

The main principle in the selection of motors are light weight and high torque, current motors rotate very fast but generate only small amounts of torque. Hence, a lightweight and efficient gearbox must be used.

The motor used is a 1000kv brushless out runner with a power of 75 W, the choice of this motor was due to the availability in the market and the cost effectiveness.

1000Kv Brushless out runner is a Brushless DC electric motor (BLDC motors) also known as electronically commutated motors (ECMs, EC motors) are synchronous motors that are powered by a DC electric source via an integrated inverter switching power supply, which produces an AC electric signal to drive the motor

Generally, out runner motors reduce the need for a gearbox, reduced the prop size range to select from, and, also reduced the range of cells that could be used for a particular motor.

These motors generate much more torque than a normal in runner motor, it's specification are in table (10).

Table 10 Motor specification

Weight	5s4 g
Battery required	Lipo-3 cells 11.1v
Revolution per volt	1000

Figure 16 Selected motor

The battery used is an 800 mah LiPo 3 cell 11.1 V battery, the battery specifications is suitable for our motor, it was also considered keeping the availability of it in the market.

Technical datasheet of this battery are in table (11).

Table 11 Battery specification

Weight	88 g
Battery type	Lipo
Number of cells	3
Capacity	800 mAh

Figure 17 The battery

4 Chapter Four: Result and Discussion

4.1 Aerodynamic result

The analysis for the model was done using CFD and analytical methods for min and max velocity and for max frequency and at different angles of attack. The lift force L and drag D were calculated by integrating the pressure and shear-wall stresses over the model surface. in unsteady aerodynamic the lift, drag and moment are change with time and the wing position during the flapping period so the lift, drag and moment were taken at the middle of the flapping stroke. Which is the max value of the force generating and that the max load as the structure must deal with. This result is for wing only without tail and fuselage for one flapping cycle as we need to calculate the lift and thrust for the model.

4.1.1 CFD result

The result from ANSYS fluent are:

4.1.1.1 Lift force at min velocity

From figure (20), the lift coefficient of the wing for one flapping cycle at velocity 5m/s start form the middle of down stroke and as we see the lift changes with time as sinusoidal curve and that is due to flapping motion. The lift starts form max value and then drop and equal to zero at the end of the down stroke and then get negative value as upstroke starts and get max negative value at the middle of upstroke and then get less negative until equal zero at the last of upstroke and the starting of down stroke. These results make sense as the model for first need lift to get in air and this lift must be as high as possible and this is why the flapping first fold down.

4.1.1.2 Drag force at min velocity

Fig (21) shows the drag coefficient of the model for one flapping cycle starting from the middle of the down stroke as we see the curve starts form the most negative value which means thrust and then get less negative until get zero at the end of down stroke and the start of upstroke the change of the drag coefficient also is sinusoidal along time like lift. From this result we can see that the model first produces thrust and then drag in order to push the model into the air for forward speed at first with no drag and that makes sense that the model need forward speed from the start.

4.1.1.3 Lift force at max velocity

The result for velocity 14m/s and angle of attack zero and one flapping cycle. Fig (22) shows the lift coefficient of the model for one flapping cycle at 14m/s and as we see

the shape of the curve is same as for velocity 5m/s the only different is that for max and min value it is more less than that for 5m/s and that due to first the increase in unsteady effect due to high forward speed and also the necessary lift need is produce by the high forward velocity.

4.1.1.4 Drag force at max velocity

Fig (23) show drag coefficient for the model at velocity 14m/s has the same shape like the one for 5m/s the curve is only different in the max and min value which is more less than for 5m/s and that is due to the decrease in the down wash at high speed

4.1.1.5 Aerodynamic force variation with time

The result for velocity 14m/s and angle of attack zero and two flapping cycle. Fig (23) and (24) show the lift and drag coefficient for two flapping cycle at 14m/s and that shows us the lift and drag shape do not change a lot with time but there is small change in the curve shape at the second cycle due to the vortex wake in the back of the wing and that affects the lift and drag for little in the cause of steady forward flapping.

To calculate the value of lift and thrust for the model taking in the middle of the stroke which is when the wing at zero-degree flapping amplitude which is the max value for the lift and thrust.

4.1.1.6 Down stroke and upstroke force

From table (12) and (13) we show the lift and drag force at the middle of up and down stroke as we see the down stroke mainly produce lift and thrust and the down stroke produce drag and negative lift that is due to the change in angle of attack for down and up motion of the wing for down stroke the angle of attack is positive and the resultant aerodynamic force vector is up and forward direction and in the down stroke the wing have negative angle of attack which produce negative lift and drag upstroke can produce little thrust if there is effective pitch in the wing and real bird produce thrust at two stroke due to effective aerodynamic motion of the wing .

4.1.2 Analytical result

The analytical equation used to calculate the lift using modify lifting line theory at gliding and for flapping at the middle of the stroke for two velocities found in chapter three the table blow shows the lift distribution on the span at gliding and for velocity 5m/s and for 14m/s.The tables (14),(15),(16),(17),(18) and fig(18),(19) show the lift distribution using modify lifting line theory for gliding and flapping at the middle of up and down stroke the result form the equation are close to the simulation and this result make good support to the that result and can give us more detail about how lift is distribute along the span. Those equations give us good observation for the unsteady effect on the span and also the effect of circulation on flapping flight.

As we see for gliding flight which is flight with fixed wing that the model has better deal with it due to airfoil shape which can work for high angle of attack and also for high negative angle of attack.

At flapping condition, we see new component of velocity and have strong effect on the lift and drag this velocity is in vertical direction due to flapping motion which make completely change in the aerodynamic of the flight and give us amazing aerodynamic efficiency which give us thrust. This flapping motion give us the thrust but cost us special shape of the airfoil that can work at high angle of attack as we see the angle of attack at the wing tip be high at positive and negative value. And the curve blow shows us the lift distribution on the span form the table above.

From above result we find that the model can produce enough lift to hold in air and also produce thrust and the down stroke is the power stroke that lift and thrust produce only in down stroke while up stroke produce negative lift and drag and the lift during down stroke in min velocity 5m/s is twice the weight of the model and that can cover the losses in lift during upstroke.

From lift eq(L=.5*ϭ*V^2*S*cl): the lift in 5m/s in down stroke =18.27N and the weight of the model = 9.81N and at upstroke the lift = -1.2N and the drag = 1.4N. the above result are for the starting of the flapping the first and second and the value get better as the flapping cycle continues due to built-up vortex at the TE of the wing and the unsteady effect get more stable

Table 12 Aerodynamic force coefficient at down stroke

Angle of attack	X velocity	Y velocity	Cl	Cd
0	5	0	1.9	-0.25
0	14	0	0.99	-0.06

Table 13 Aerodynamic force coefficient at upstroke

Angle of attack	X velocity	Y velocity	Cl	Cd
0	5	0	-0.13	0.15
0	14	0	-0.085	.091

J	0	1	2	3	4	5	6	7	8	9	10
N	10	10	10	10	10	10	10	10	10	10	10
y/s	0.0	0.1	0.2	0.3	0.4	0.5	0.6	0.7	0.8	0.9	1.0
v-G	4.9	4.9	4.9	4.90	4.9	4.9	4.9	4.9	4.9	4.9	4.9
Γ-mG	0.82	0.82	0.82	0.82	0.82	0.82	0.82	0.82	0.82	0.82	0.82
y-ΓG	0.424	0.424	0.424	0.424	0.424	0.424	0.424	0.424	0.424	0.424	0.424
Γ-G(y)	1.04	1.04	1.02	1.00	0.96	0.90	0.84	0.75	0.63	0.46	0.00
c-aG(y)	1.27	1.27	1.25	1.21	1.17	1.10	1.02	0.91	0.76	0.55	0.00
F-QG(y)	6.2	6.2	6.1	6.0	5.7	5.4	5.0	4.5	3.7	2.7	0.00
α-G(y)	0.5	0.5	0.3	-0.1	-0.6	-1.3	-2.2	-3.3	-4.9	-7.1	-13.0
v-iG(y)	0.26	0.26	0.26	0.26	0.26	0.26	0.26	0.26	0.26	0.26	0.26
α- iG(y)	3.1	3.1	3.1	3.1	3.1	3.1	3.1	3.1	3.1	3.1	3.1
α-EG(y)	3.6	3.5	3.3	3.0	2.5	1.8	0.9	-0.3	-1.8	-4.0	-9.9

Table 14 Span wise lift at gliding

Table 15 Span wise lift at middle of upstroke 5m/s

v_K	5.0	5.0	5.0	5.0	5.0	5.0	5.0	5.0	5.0	5.0	5.0
ω_max	9.88	9.88	9.88	9.88	9.88	9.88	9.88	9.88	9.88	9.88	9.88
y_Γ1	0.000	0.000	0.000	0.000	0.000	0.000	0.000	0.000	0.000	0.000	0.000
k_Γ1	0.248	0.248	0.248	0.248	0.248	0.248	0.248	0.248	0.248	0.248	0.248
Γ_m1	0.20	0.20	0.20	0.20	0.20	0.20	0.20	0.20	0.20	0.20	0.20
Γ_1(y)	0.78	0.73	0.62	0.48	0.32	0.16	0.01	-0.13	-0.22	-0.25	0.00
v_u1(y)	0.0	1.0	2.0	3.0	4.0	4.9	5.9	6.9	7.9	8.9	9.9
v_e1(y)	5.0	5.1	5.4	5.8	6.4	7.0	7.7	8.5	9.3	10.2	11.1
c_a1(y)	0.93	0.85	0.69	0.49	0.30	0.14	0.01	-0.09	-0.14	-0.15	0.00
F_Q1[y]	4.7	4.5	4.1	3.4	2.5	1.4	0.1	-1.3	-2.6	-3.1	0.0
α_1(y)	-3.1	-3.9	-5.7	-7.8	-9.8	-11.5	-12.9	-13.9	-14.5	-14.6	-13.0
v_i1(y)	0.58	0.46	0.34	0.22	0.09	-0.03	-0.15	-0.27	-0.39	-0.52	-0.64

α_i1(y)	6.7	5.2	3.6	2.1	0.9	-0.2	-1.1	-1.8	-2.4	-2.9	-3.3
δ_1(y)	0.0	11.2	21.7	30.8	38.5	44.8	50.0	54.3	57.8	60.8	63.3
α_E1(y)	3.6	12.5	19.6	25.2	29.5	33.0	35.9	38.5	40.9	43.3	47.0

Table 16 Span wise lift at middle of down stroke for 5m/s

y_Γ2	0.481	0.481	0.481	0.481	0.481	0.481	0.481	0.481	0.481	0.481	0.481
k_Γ2	1.735	1.735	1.735	1.735	1.735	1.735	1.735	1.735	1.735	1.735	1.735
Γ_m2	1.42	1.42	1.42	1.42	1.42	1.42	1.42	1.42	1.42	1.42	1.42
Γ_2(y)	1.33	1.37	1.44	1.51	1.58	1.63	1.64	1.58	1.44	1.13	0.00
v_u2(y)	0.0	-1.0	-2.0	-3.0	-4.0	-4.9	-5.9	-6.9	-7.9	-8.9	-9.9
v_e2(y)	5.0	5.1	5.4	5.8	6.4	7.0	7.7	8.5	9.3	10.2	11.1
c_a2(y)	1.59	1.60	1.60	1.56	1.48	1.38	1.26	1.11	0.92	0.66	0.00
F_Q2[y]	8.1	8.5	9.4	10.7	12.3	14.0	15.5	16.5	16.5	14.1	0.0
α_2(y)	3.9	4.1	4.0	3.5	2.8	1.7	0.4	-1.2	-3.2	-6.0	-13.0
v_i2(y)	-0.03	0.08	0.20	0.31	0.43	0.54	0.65	0.77	0.88	0.99	1.11
α_i2(y)	-0.3	1.0	2.1	3.1	3.8	4.4	4.8	5.1	5.4	5.6	5.7
δ_2(y)	0.0	-11.2	-21.7	-30.8	-38.5	-44.8	-50.0	-54.3	-57.8	-60.8	-63.3
α_E2(y)	3.6	-6.2	-15.5	-24.2	-31.9	-38.7	-44.8	-50.4	-55.7	-61.2	-70.6
V_Δα2	-81.0										
V_ΔαK	143.5										

Table 17 Span wise lift at middle of upstroke for 14m/s

v_K	13.7	13.7	13.7	13.7	13.7	13.7	13.7	13.7	13.7	13.7	13.7
ω_max	9.88	9.88	9.88	9.88	9.88	9.88	9.88	9.88	9.88	9.88	9.88
y_Γ1	0.000	0.000	0.000	0.000	0.000	0.000	0.000	0.000	0.000	0.000	0.000
k_Γ1	0.682	0.682	0.682	0.682	0.682	0.682	0.682	0.682	0.682	0.682	0.682
Γ_m1	0.56	0.56	0.56	0.56	0.56	0.56	0.56	0.56	0.56	0.56	0.56
Γ_1(y)	2.14	2.00	1.70	1.32	0.89	0.44	0.02	-0.35	-0.61	-0.69	0.00

v_u1(y)	0.0	1.0	2.0	3.0	4.0	4.9	5.9	6.9	7.9	8.9	9.9
v_e1(y)	13.7	13.7	13.8	14.0	14.2	14.5	14.9	15.3	15.8	16.3	16.9
c_a1(y)	0.93	0.87	0.73	0.56	0.37	0.18	0.01	-0.14	-0.23	-0.25	0.00
F_Q1[y]	35.8	33.5	28.8	22.6	15.5	7.9	0.4	-6.6	-11.9	-13.7	0.0
α_1(y)	-3.1	-3.8	-5.2	-7.0	-9.1	-11.1	-12.9	-14.4	-15.5	-15.7	-13.0
v_i1(y)	1.60	1.27	0.93	0.60	0.26	-0.08	-0.41	-0.75	-1.08	-1.42	-1.75
α_i1(y)	6.7	5.3	3.9	2.4	1.0	-0.3	-1.6	-2.8	-3.9	-5.0	-5.9
δ_1(y)	0.0	4.1	8.2	12.2	16.1	19.9	23.4	26.8	30.0	33.0	35.9
α_E1(y)	3.6	5.6	6.9	7.6	8.1	8.5	8.9	9.6	10.7	12.4	16.9
V_Δα1	13.4										

Table 18 Span wise lift at middle of upstroke for 14m/s

y_Γ2	0.481	0.481	0.481	0.481	0.481	0.481	0.481	0.481	0.481	0.481	0.481
k_Γ2	4.769	4.769	4.769	4.769	4.769	4.769	4.769	4.769	4.769	4.769	4.769
Γ_m2	3.91	3.91	3.91	3.91	3.91	3.91	3.91	3.91	3.91	3.91	3.91
Γ_2(y)	3.66	3.76	3.95	4.16	4.35	4.47	4.50	4.35	3.96	3.10	0.00
v_u2(y)	0.0	-1.0	-2.0	-3.0	-4.0	-4.9	-5.9	-6.9	-7.9	-8.9	-9.9
v_e2(y)	13.7	13.7	13.8	14.0	14.2	14.5	14.9	15.3	15.8	16.3	16.9
c_a2(y)	1.59	1.63	1.70	1.77	1.82	1.83	1.80	1.69	1.49	1.13	0.00
F_Q2[y]	61.2	63.1	66.8	71.2	75.8	79.7	82.0	81.7	76.5	61.8	0.0
α_2(y)	3.9	4.4	5.1	5.8	6.3	6.5	6.1	5.0	2.9	-1.0	-13.0
v_i2(y)	-0.08	0.23	0.55	0.86	1.17	1.48	1.79	2.10	2.42	2.73	3.04
α_i2(y)	-0.3	1.0	2.3	3.5	4.7	5.8	6.9	7.8	8.7	9.5	10.2
δ_2(y)	0.0	-4.1	-8.2	-12.2	-16.1	-19.9	-23.4	-26.8	-30.0	-33.0	-35.9
α_E2(y)	3.6	1.2	-0.9	-2.9	-5.1	-7.6	-10.5	-14.0	-18.5	-24.5	-38.6
V_Δα2						-18.7					
V_ΔαK						32.1					

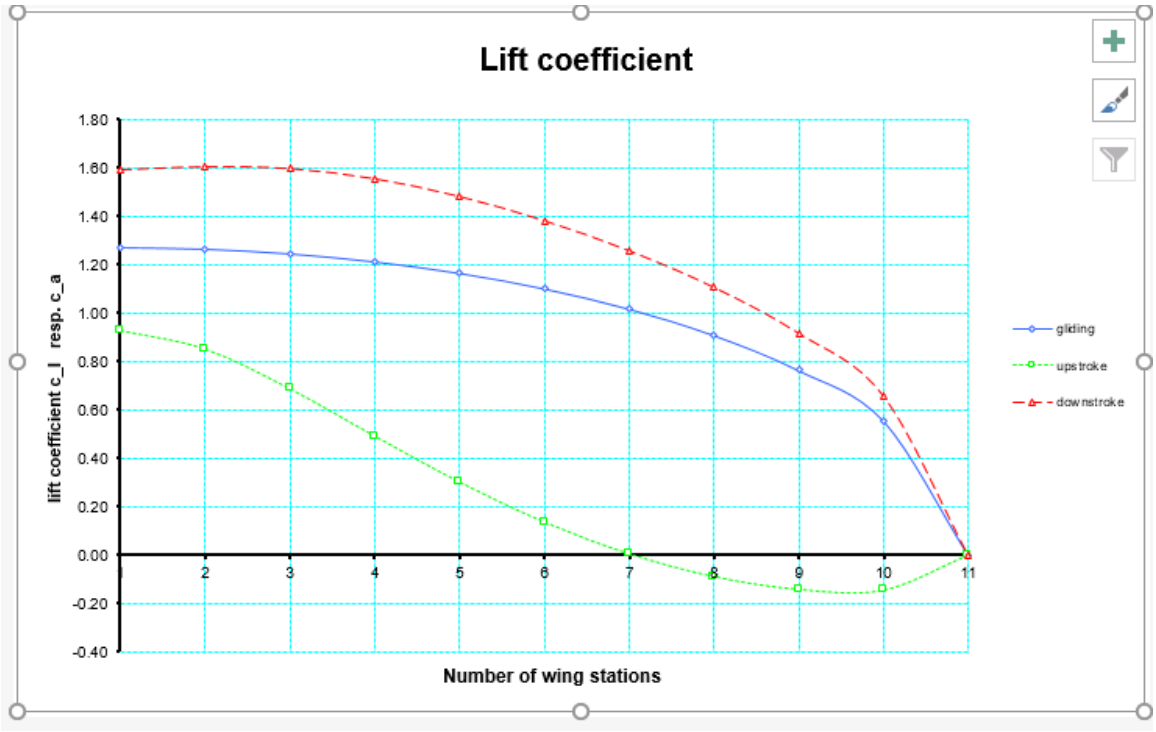

Figure 18 Span wise lift for v=5 m/s

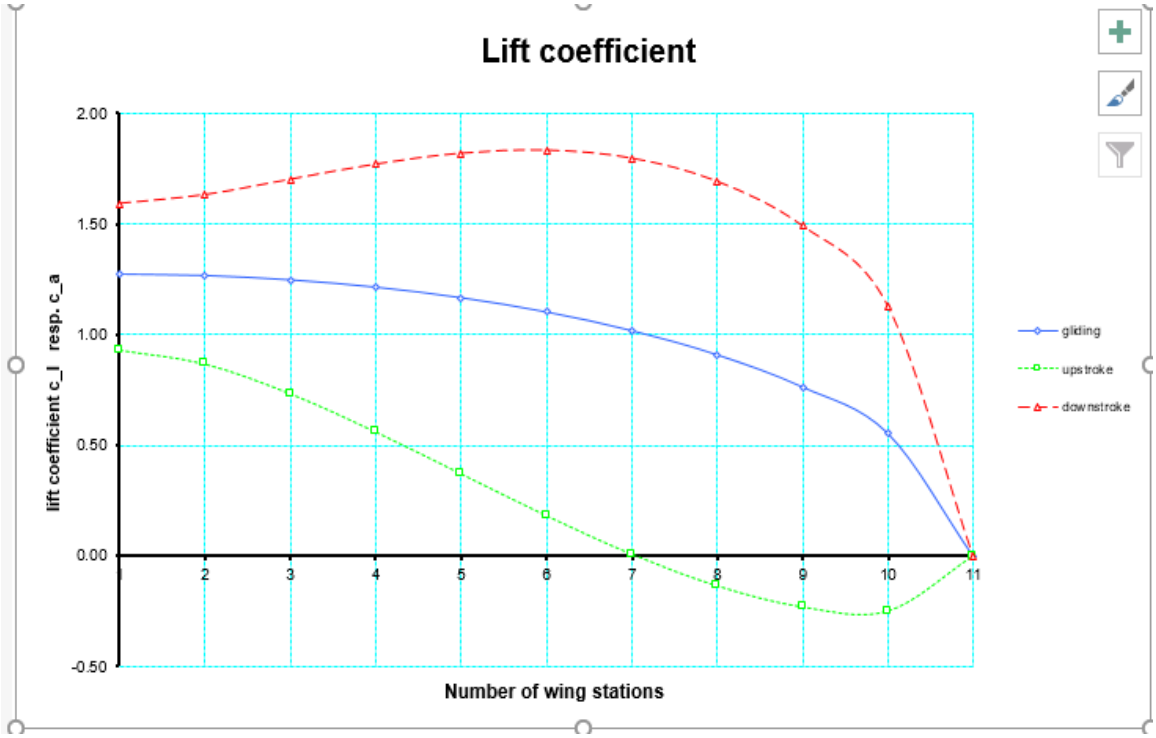

Figure 19 Span wise lift for 14m/s

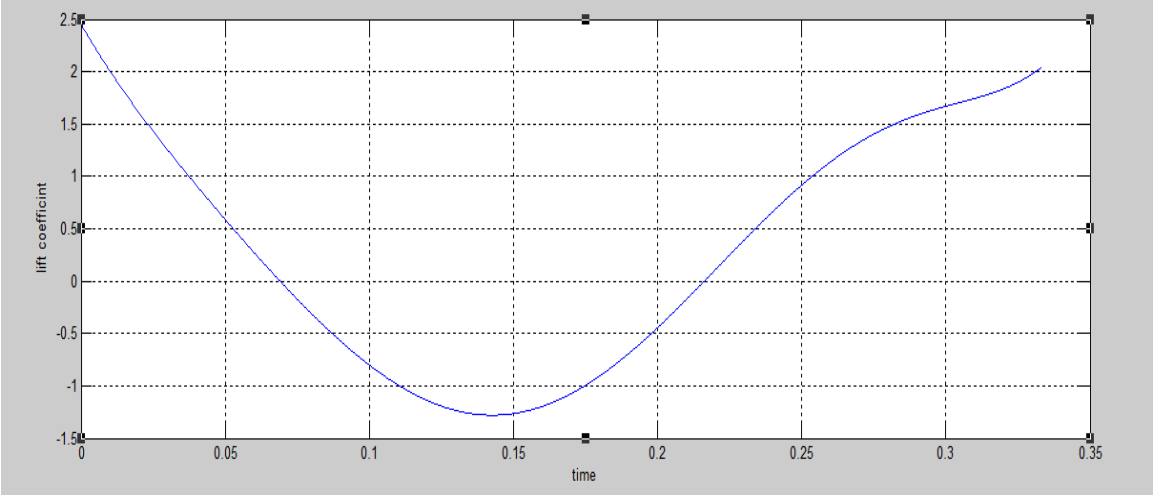

Figure 20 Lift coefficient for 5m/s

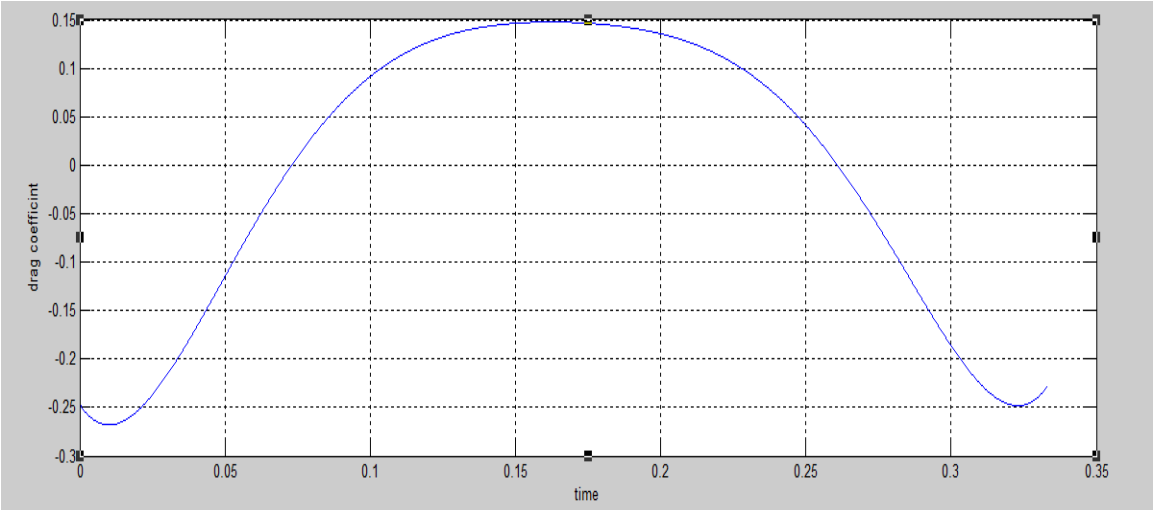

Figure 21 Drag coefficient for 5m/s

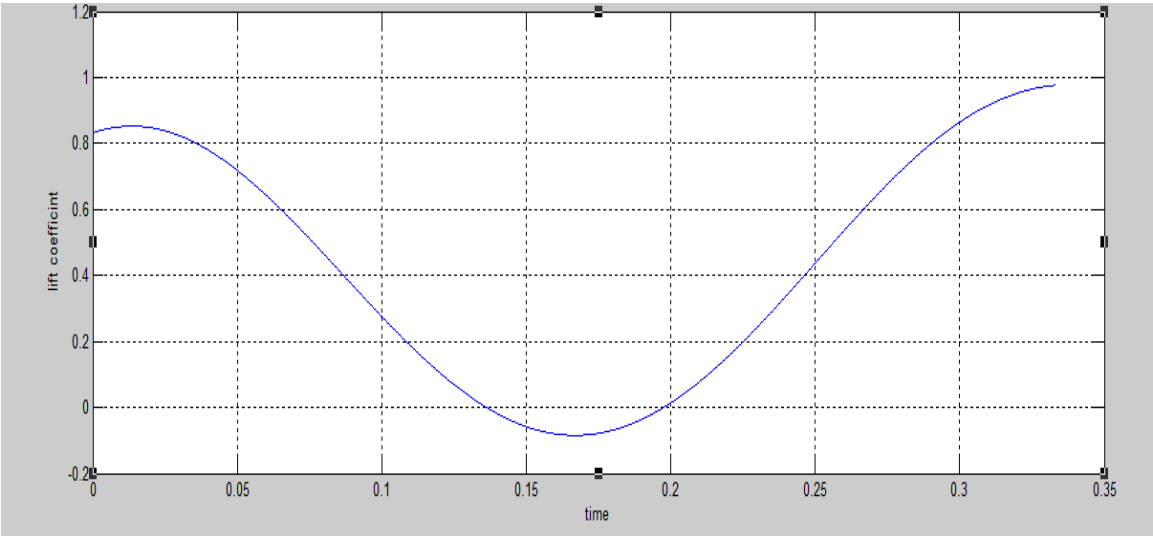

Figure 22 Lift coefficient for 14m/s

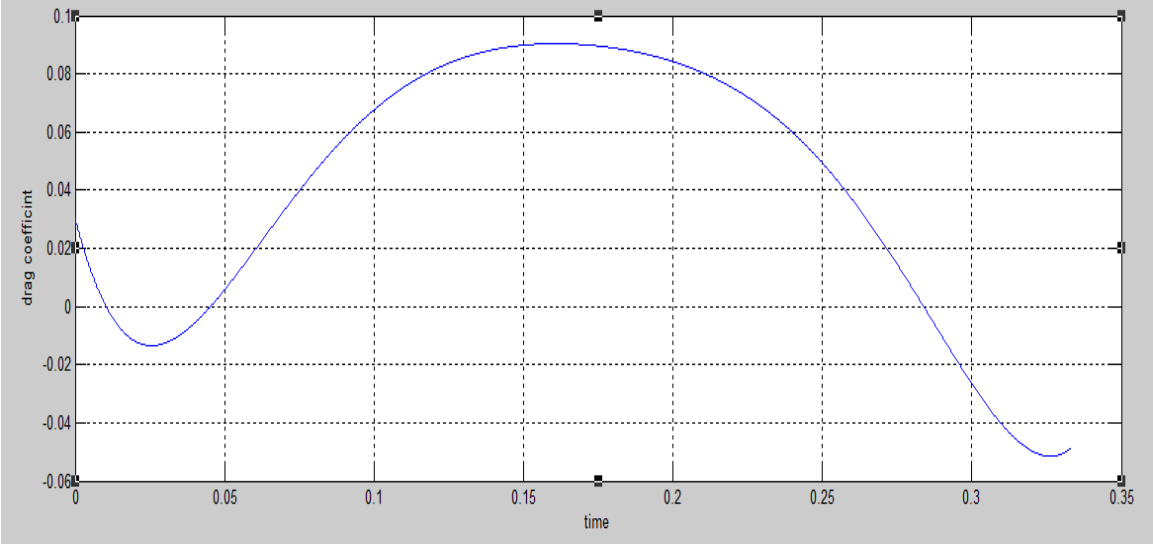

Figure 23 Drag coefficient for 14m/s

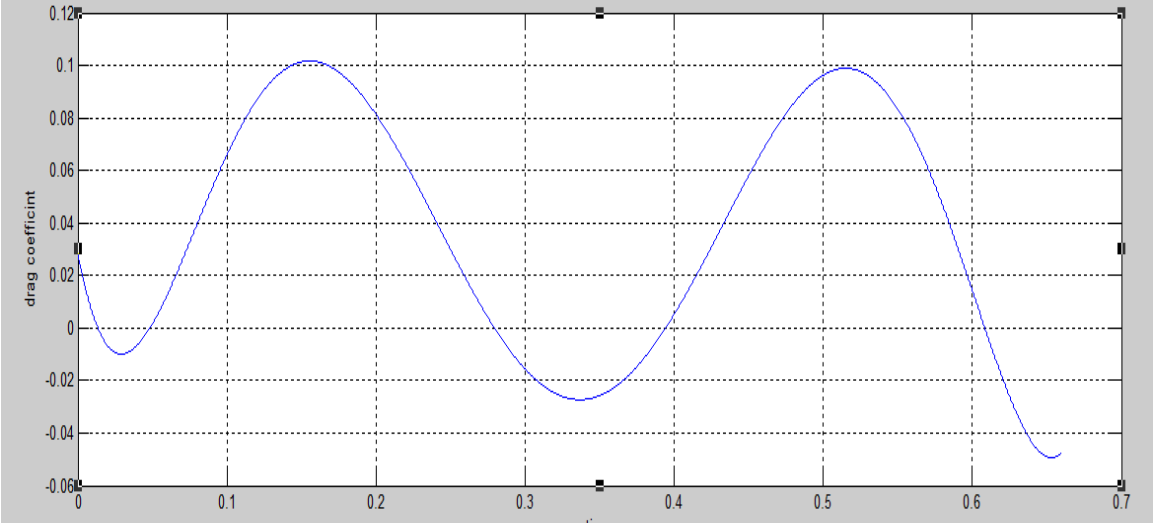

Figure 24 Drag coefficient for two flapping cycle

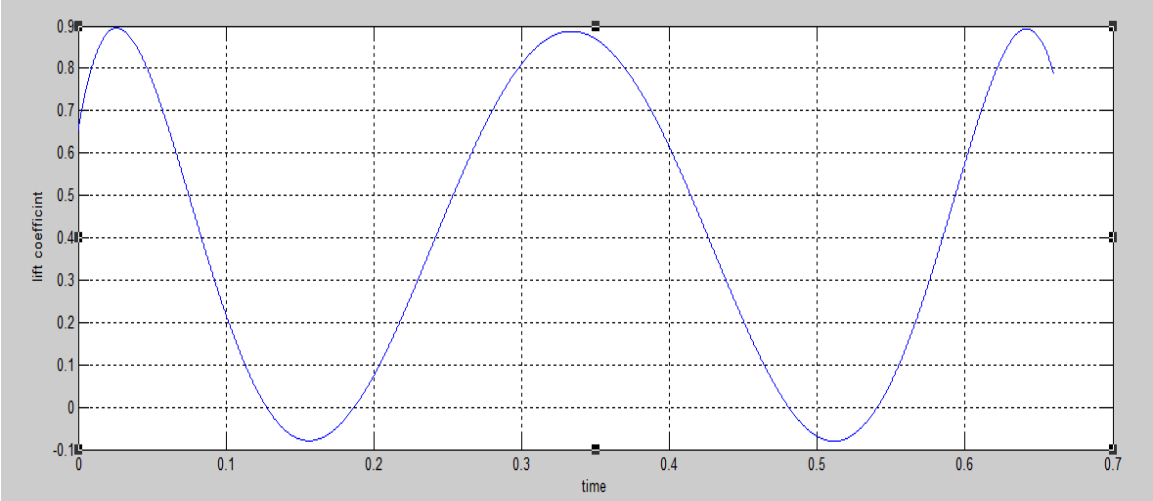

Figure 25 Lift coefficient for two flapping cycle

4.1.3 **Flow velocity Path lines in the end of upstroke and down stroke**

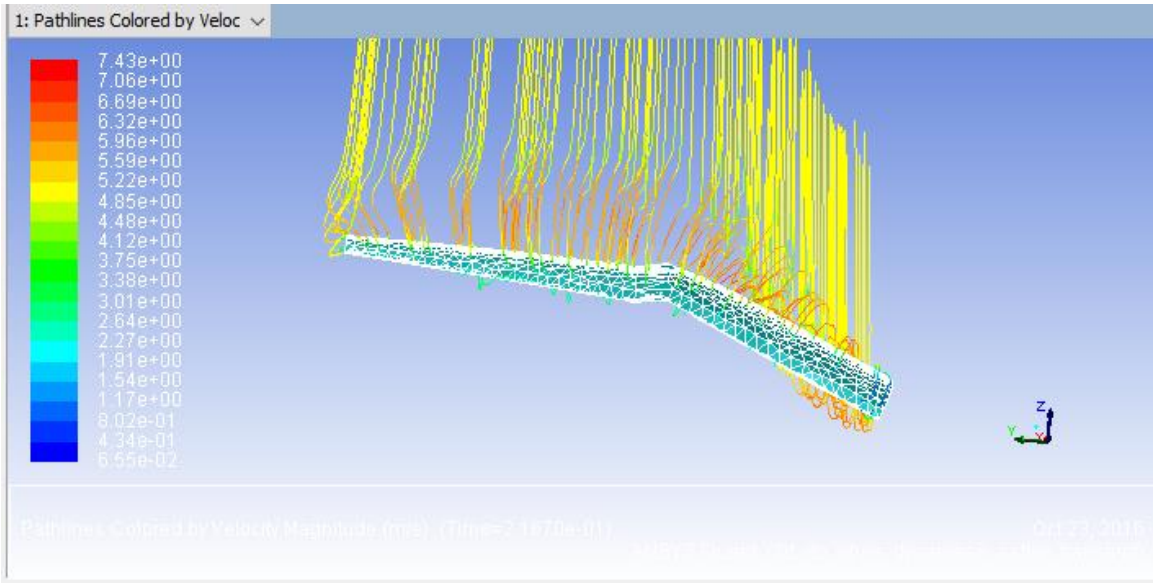

Figure 26 Flow path line at end of upstroke

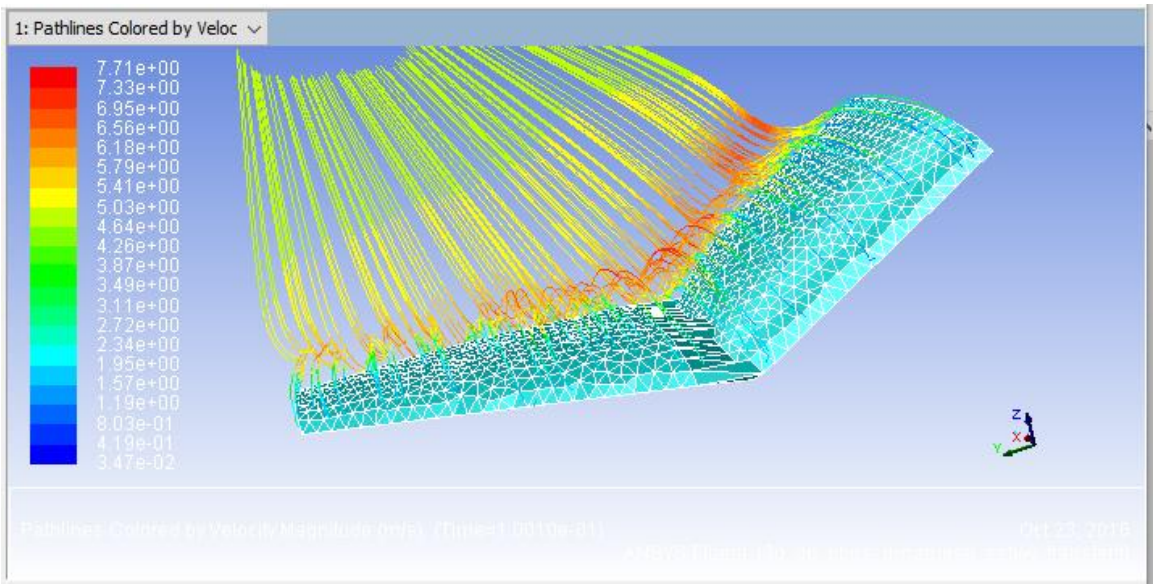

Figure 27 Velocity path line at end of down stroke

4.2 Structure Result

After applying Finite element analysis to the structure, the results prove that the model structure is strong enough and suitable to carry the aerodynamic and mechanical loads subjected to the aircraft.

The dark blue color indicates the minimum deformation of the spar which is at the root –(zero length) where the spar is fixed-, and the color gradating continue until dark red which indicates maximum deformation at the free end of the spar.

4.2.1 External spar deformation in gliding

Gliding can be considered as the phase of minimum loading because the wing is at its neutral position and there is no flapping motion as shown in figure (25).

4.2.2 External spar deformation in up stroke at v = 14 m/s

Due to high speed and its position in the wing, the external spar examines little high deformation but this deformation still not redounded.

During upstroke phase there is no significant aerodynamic load, hence, this deformation is due to mechanical loading and spar weight. This deformation can be useful because during flapping motion the A.O.A is not constant along the span, hence the deformation can be used as flexibility feature to the spar and same thing for thrust generation as shown in figure (26)

4.2.3 External spar deformation up stroke at v = 5 m/s

Due to low loads during upstroke, the maximum deformation is small and does not affect the normal behavior of the spar. we can note that the maximum deformation is high relative to the speed, that is because of its position in the wing and its relatively small dimension. This is shown in figure (27).

4.2.4 Internal spar deformation in gliding

Due to its fixation to the fuselage and its bigger dimension, the internal spar examines very small deformation specially in gliding phase where the aerodynamic and mechanical loading may be considered to be the minimum as shown in figure (28).

4.2.5 Internal spar deformation in up stroke at v = 5 m/s

The maximum deformation is very small because of minimum speed and low aerodynamic load in up stroke phase and this deformation does not affect the normal behavior of the spar and can be neglected as shown in figure (29).

4.2.6 **Internal spar deformation in upstroke at v = 14 m/s**

Because of high speed, the maximum deformation increases but not to unacceptable level. This level of deformation can affect the normal operation of the mechanism of the external spar because rod (B) which transfers the motion from the motor to the external spar is fixed to the internal spar. As shown in figure (30).

4.2.7 **internal spar deformation in down stroke at v = 5 m/s**

Down stroke is the phase of lift creation, and hence even the minimum speed creates a deformation but this deformation is small and can be neglected. this is shown in figure (31).

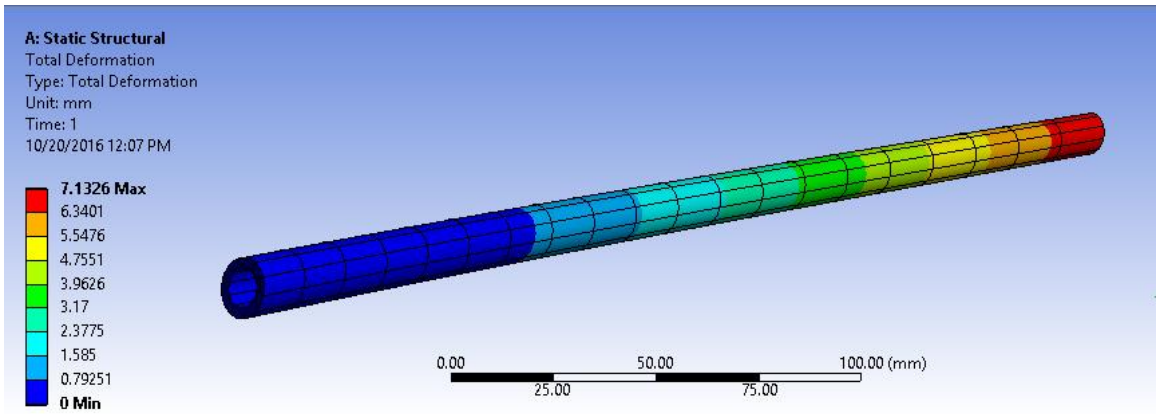

Figure 28 External spar deformation in gliding

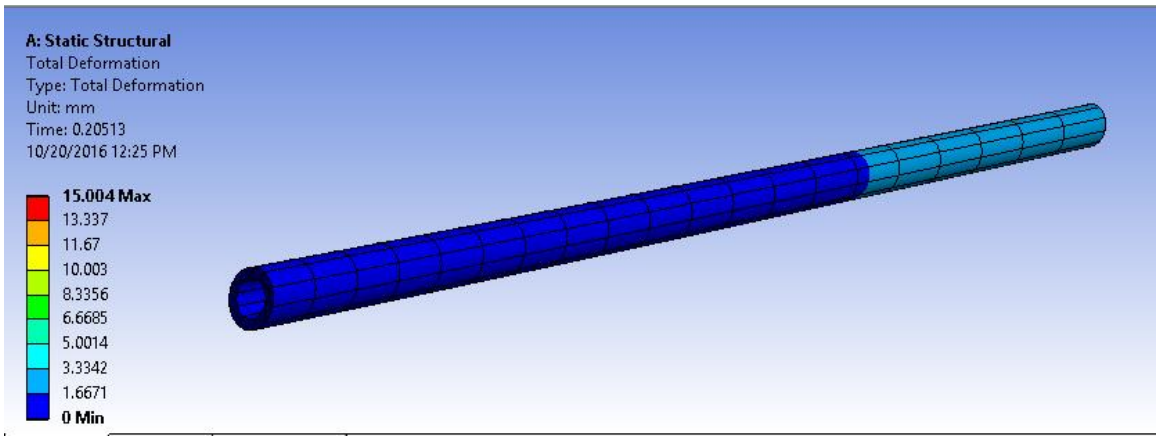

Figure 29 External spar deformation in up stroke at v = 14 m/s

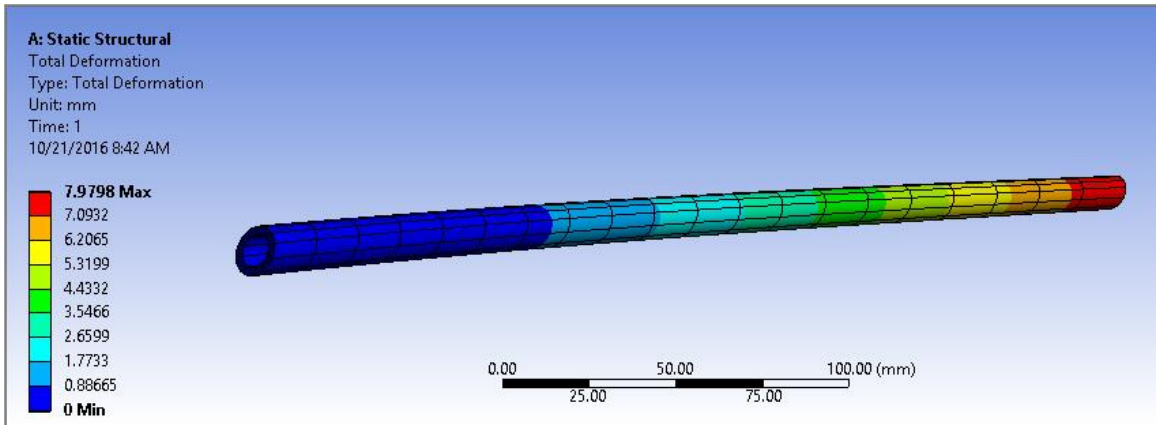

Figure 30 External spar deformation up stroke at v = 5 m/s

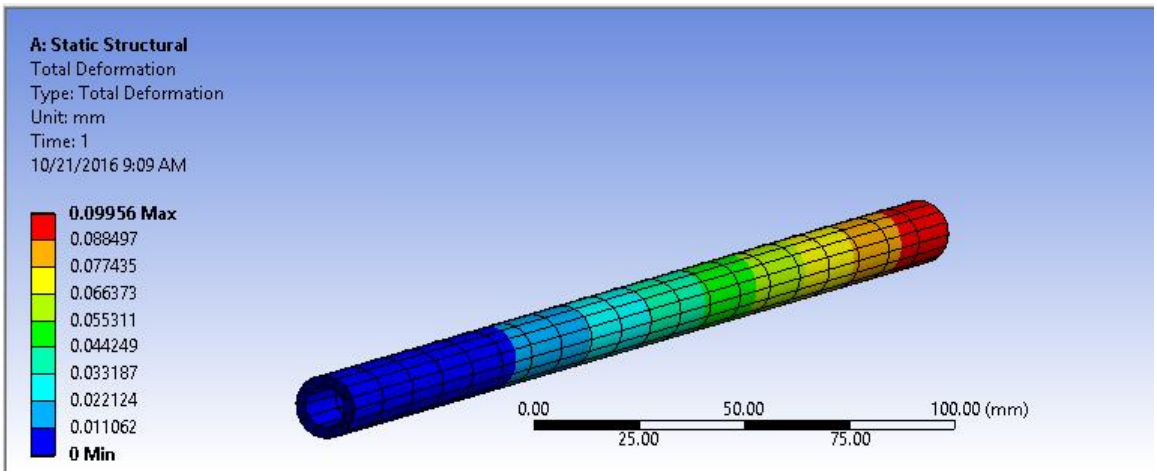

Figure 31 Internal spar deformation in gliding

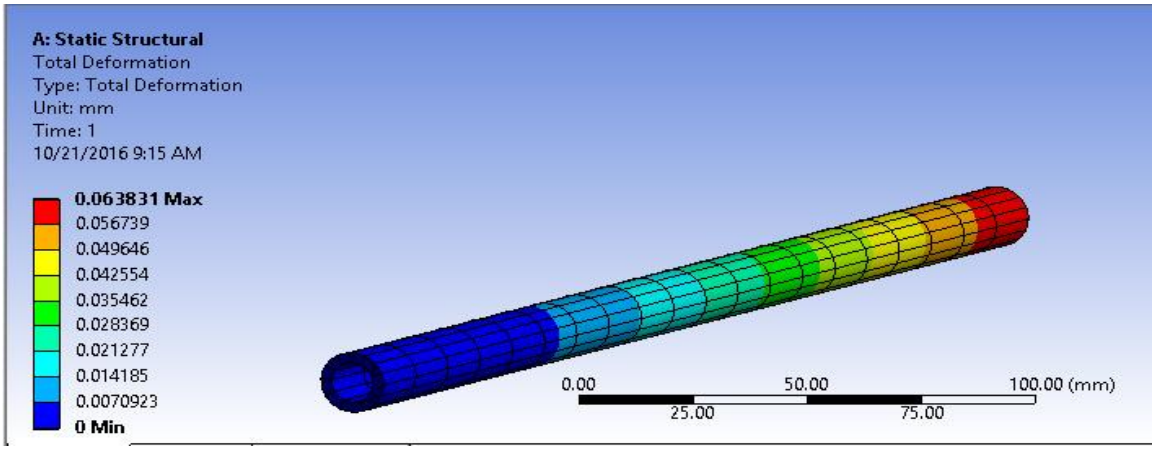

Figure 32 Internal spar deformation in up stroke at v = 5 m/s

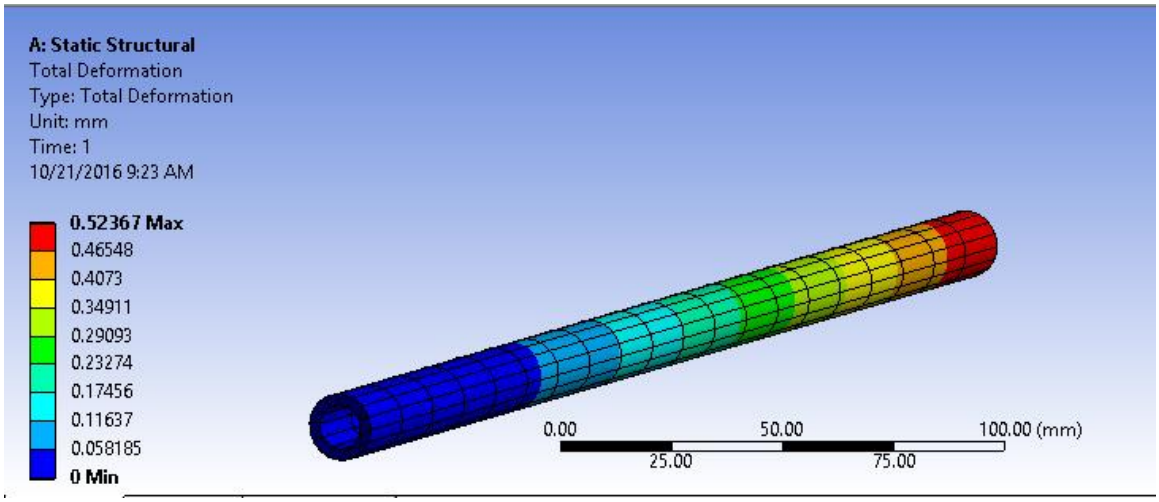

Figure 33 Internal spar deformation in upstroke at v = 14 m/s

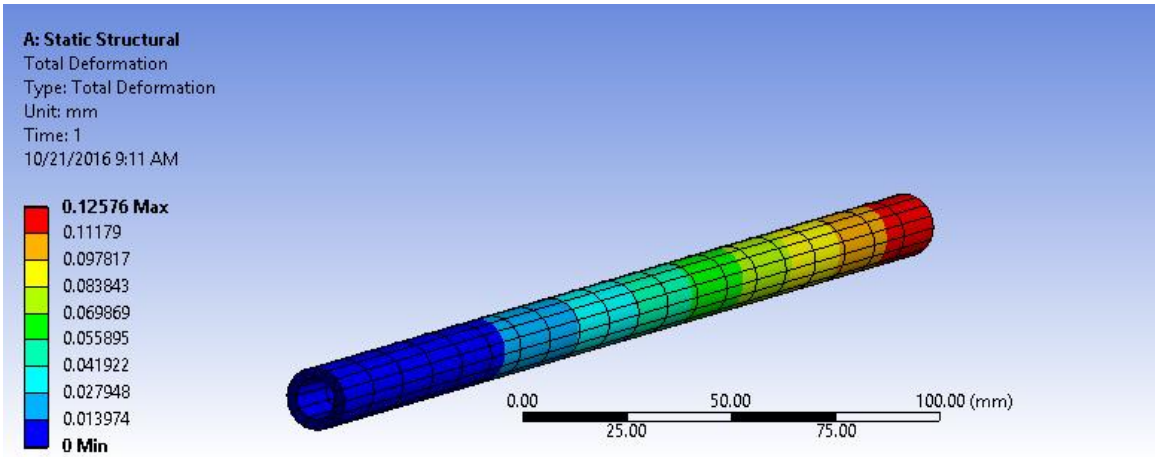

Figure 34 Internal spar deformation in down stroke at v = 5 m/s

5 Chapter five: Conclusion and Recommendation

5.1 Conclusion

The problem of flying in low Re number region was solved in this project by using a propulsion system which generates both lift and thrust from the wing.

The configuration was chosen to be similar to the sea-gull and was drawn using CATIA, then the aerodynamic characteristics of the model was estimated using analytical and CFD methods, the CFD results showed that the model can generate the required lift and thrust to achieve the sustainable flight. Then structure analysis was performed using ANSYS software and the result proved that the structure behavior is within acceptable limits and can handle with the subjected loads without failure or any undesired behavior.

Depending on aerodynamic and structure analysis, the mechanism -which is able to create desired flapping motion- was designed to create required lift and thrust.

5.2 Recommendation

We recommend that:

- To go deep in understanding of unsteady aerodynamics as it is so difficult.
- To use experimental method for more accurate result.
- To use smart material in order to improve structure behave.
- Study flapping motion effect on CG.
- Diagnostic and solve the problem of skewness being one when analyze the wing with its skin.

5.3 Future work

- Stability and control.
- Manufacture and test the model.
- Complete the system selection installation (Autopilot, GPS, Camera, etc.)

6 Appendix A

UDF code:

```
#include "udf.h"

DEFINE_CG_MOTION(wing_internal, dt, vel, omega, time, dtime)
{
real a1, a2, w, pi;

pi = 3.141592654;

/* define motion variables */
  a1 = 30 * pi / 180; /* 30 degree flapping amplitude */
  a2 = 30 * pi / 180; /* 30 degree feathering amplitude */
  w = 2 * pi * 3; /* 3 Hz frequency */

/* define wing rotational motion in stationary coordinates */
  omega[0] =  -a1 * w * cos(w*time);    /* flapping speed */

}



#include "udf.h"

DEFINE_CG_MOTION(wing_external, dt, vel, omega, time, dtime)
{
```

```
real   lcg=.2333;
 real  pi = 3.141592654;
real   lin=0.3833;
 real   lgap=0.0333;

  real a1 = 30 * pi / 180;
   real a2 = 50 * pi / 180;

 real w = 2 * pi * 3;



 real B=1;
 real  C=1.1963;




 real  drollin=a1*w*cos(w*time);
```

7 Appendix B

Wing motion code:

```
clc
clear all
lcg=.2333;
pi = 3.141592654;
lin=0.3833;
lgap=0.0333;

  a1 = 30 ;
    a2 = 50 ;

  w = 2 * pi * 3;
t=0:.01:1;

  B=1;
   C=1.1963;

 %%


drollin=a1*w*cos(w*t);
drollex=(a2*w*sin(w*t).*exp(B*sin(2*w*t-pi/2)-B))/C;


rollex=(-a2*(pi/2)*erf(2^(.5)*B^(.5)*cos(w*t)))/(2*B^(.5)*C);
rollin=a1*sin(w*t);
rollex1=(-a2*(pi/2)*(2^(5)*B^(5)*cos(w*t)))/(2*B^(5)*C);

plot(t,rollin,t,rollex)
%%

 zi=(1.0.*(lin+lgap).*cos(rollin));
 yi=(-1.0.*(lin+lgap).*sin(rollin));


dzi=-1.0*(lin+lgap).*sin(rollin).*drollin;
dyi=-1.0*(lin+lgap).*cos(rollin).*drollin;
%%


z=1.0*lcg*cos(rollin+rollex).*180/pi;
y=-1.0*lcg*sin(rollin+rollex).*180/pi;

dz=-1.0.*lcg.*sin(rollin+rollex).*(drollin+drollex);
dy=-1.0.*lcg.*cos(rollin+rollex).*(drollin+drollex);

z1=1.0*lcg*cos(rollin+rollex1).*180/pi;
y1=-1.0*lcg*sin(rollin+rollex1).*180/pi;
```

8 Appendix C

Acceleration of gravity	g	m/s^2	9.81
Air density	ρ	kg/m^3	1.225
Mass of model	m_M	kg	1.00
Span	b	m	2.00
Chord (rectangular planform)	l	m	0.336
Angle of attack for zero lift	α_0	deg	-13
Angle to tangent of lower surface	σ	deg	0.0
Flapping period length (sinusoidal)	t_p	s	0.333
Flapping angle (± middle of stroke)	Φ_E	deg	30

9 References

1. Han, J.-H., J.-S. Lee, and D.-K. Kim. *Bio-inspired flapping UAV design: a university perspective*. in *SPIE Smart Structures and Materials+ Nondestructive Evaluation and Health Monitoring*. 2009. International Society for Optics and Photonics.
2. Viieru, D., et al., *Flapping and flexible wing aerodynamics of low Reynolds number flight vehicles.* AIAA paper, 2006. **503**: p. 2006.
3. Shyy, W., et al., *Aerodynamics of low Reynolds number flyers*. Vol. 22. 2007: Cambridge University Press.
4. Yu, C., D. Kim, and Y. Zhao, *Lift and Thrust Characteristics of Flapping Wing Aerial Vehicle with Pitching and Flapping Motion.* Journal of Applied Mathematics and Physics, 2014. **2**(12): p. 1031.
5. Guerrero, J.E., et al., *Preliminary design of a small-sized flapping UAV. II. Aerodynamic Performance and Flight Stability.* Convegno AIMETA, 2013.
6. Robertson, C.D. and T.M. Reichert, *Design and development of the atlas human-powered helicopter.* AIAA Journal, 2014. **53**(1): p. 20-32.
7. Norizham, A.R. and G. Dimitriadis, *Flapping flight aerodynamics for flying animals.* 2011.
8. Yonggang, Y., X. Youzeng, and H. Lipeng, *Design and Research on Mechanism of Bionic Flapping-wing Air Vehicle.* International Journal of Hybrid Information Technology, 2015. **8**(4): p. 299-306.
9. Malik, M.A. and F. Ahmad. *Effect of Different Design Parameters on Lift, Thrust, and Drag of an Ornithopter*. in *Proceedings of the World Congress on Engineering*. 2010.
10. Djojodihardjo, H., A.S.S. Ramli, and S. Wiriadidjaja, *Kinematic and aerodynamic modelling of flapping wing ornithopter.* Procedia Engineering, 2012. **50**: p. 848-863.
11. Hu, H., et al., *An experimental investigation on the aerodynamic performances of flexible membrane wings in flapping flight.* Aerospace Science and Technology, 2010. **14**(8): p. 575-586.
12. Räbiger, H., *Wie Ornithopter fliegen*. 2002: Horst Räbiger.
13. BOTTARO, C.M.P.A., D.I.J. GUERRERO, and F. VECCHIA, *STUDY ON SKYBIRD PERFORMANCE IMPROVEMENT*.
14. Räbiger, H., *Lift during wing upstroke.*
15. Ma, R., et al. *Multi-objective optimization design of low-Reynolds-number airfoils S1223*. in *27th International Congress of the Aeronautical Sciences*. 2010.